

General Spin Analysis from Angular Correlations in Two-Body Decays

Seong Youl Choi*, Jae Hoon Jeong†, and Ji Ho Song‡

Department of Physics and RIPC, Chonbuk National University, Jeonju 54896, Korea

(March 4, 2019)

Abstract

Determining the spin of any new particle and measuring its couplings to other particles and/or itself are crucial in reconstructing the structure of any quantum field theory containing the particle. A general helicity formalism is employed to describe the polarization of the particle Y in a two-body decay $X_2 \rightarrow YX_1$ with polarized X_2 for the purpose of diagnosing the dynamical properties of three involved particles and for determining their spins altogether. We perform a general and comprehensive analytic analysis with our special focus on grasping fully how to connect the decay helicity amplitudes and decay distributions in the X_2 rest frame and those in a laboratory frame with X_2 moving with a non-zero velocity through Wick helicity rotation on helicity states and amplitudes. This theoretical framework is demonstrated in a detailed illustrative manner with the Standard Model (SM) processes, the sequential process $e^-e^+ \rightarrow Z \rightarrow \tau^-\tau^+$ followed by $\tau^- \rightarrow \rho^-\nu_\tau \rightarrow (\pi^-\pi^0)\nu_\tau$ and the sequential process $e^-e^+ \rightarrow t\bar{t}$ followed by $t \rightarrow W^+b \rightarrow (\ell^+\nu_\ell)b^-$, and one non-standard decay process of a new vectorlike heavy top quark, $T \rightarrow Zt$, followed by $Z \rightarrow \ell^-\ell^+$. All the useful formulas directly applicable to any combinations of spins and any types of couplings in the two-body decay $X_2 \rightarrow YX_1$ followed by suitable Y two-body decays processes are collected and described in detail.

1 Introduction

Along with mass, spin is a basic invariant property that every elementary particle and any isolated object must possess in the four-dimensional spacetime with Lorentz invariance [1]. Questions and answers about the spin dependence of reactions therefore have played an essential role in probing the underlying theoretical structures very deeply and therefore establishing the SM of electroweak and strong interactions in elementary particle physics up to now [2–4].

On the high energy frontier, equipped with the Large Hadron Collider (LHC) [5], we are now probing the electroweak (EW) scale ($v = 246$ GeV) and beyond intensively and extensively after having established the SM by the decisive discovery of a Higgs boson [6, 7] followed by very precise measurements of its mass and couplings [8, 9] and model-independent determinations of its spinless nature [10–15]. The true theory for the origin and stability of the EW scale [16–19] beyond the SM is highly expected to be revealed with a huge amount of accumulated data.

One generic prediction in most of new models is the presence of new particles partnered with some or all of the SM particles. For instance, every SM particle in low-energy supersymmetry (SUSY) [20–25] has a

*choisy7@gmail.com
†jeong229@jbnu.ac.kr
‡sonjih0@nate.com

heavier partner whose spin differs by $1/2$ in units of \hbar . Alternatively, in universal extra dimension (UED) models [26,27], each SM particle is paired with a tower of Kaluza-Klein (KK) excitations with identical spin. Thus, model-independent determinations and detailed measurements of the spins and dynamical structures are crucial in discriminating among new scenarios.

In the present work a general theoretical framework is presented for describing the spin and polar-angle correlations¹ in the two-stage two-body decays of a polarized state X_2 of spin j_2 and mass m_2 into two on-shell states, Y of spin j and mass m and X_1 of spin j_1 and mass m_1

$$X_2[j_2, m_2] \rightarrow Y[j, m] + X_1[j_1, m_1], \quad (1)$$

followed by a two-body decay of the particle Y into a particle a of spin j_a and mass m_a and a particle b of spin j_b and mass m_b

$$Y[j, m] \rightarrow a[j_a, m_a] + b[j_b, m_b], \quad (2)$$

where at least the momentum of the particle a is assumed to be measurable event by event.² For a non-zero j_2 , the X_2 particle is produced generally in a polarized state in its production processes, in particular, if the interactions are parity-violating, and the polarization of the particle Y with a non-zero spin j can be extracted (partially) through the angular distributions in its sequential decays. If the branching fractions are sizable, then the sequential two-stage decays can provide us with a powerful tool not only for examining the properties of the involved particles but also for determining their spins altogether, as will be demonstrated with specific examples in the following.

When the rest frame of the decaying particle is hardly reconstructible as in pp collisions at the LHC, the direct spin measurements are performed conventionally through a set of Lorentz-invariant masses constructed in sufficiently long decay chains [29–31]. Such spin-determination methods tend to rely heavily on a number of final state spins and involved (chiral) couplings [32,33]. In this work, we will demonstrate with several specific examples that the polar-angle correlations of the Y in the rest frame of X_2 (X_2RF) and one of the Y decay products in the Y rest frame (assumed to be reconstructed at least partially) also enable us to determine the spins and underlying dynamics decisively and clearly.

If the four-momentum of the particle Y or one of its decay products can be determined event by event even though the momentum of the decaying parent particle X_2 is not reconstructed, one natural reference axis for describing the Y polarization is nothing but the Y flight direction *in the laboratory frame (LAB)*, to be called the detection axis in the following. In this situation, the most natural experimental observable for Y decays is then the polar-angle as well as azimuthal-angle distribution of one of the Y decay products in the Y rest frame *boosted back directly along the Y momentum direction in the LAB*.

Certainly, the most convenient reference system for describing the dynamics of the two-body decay $X_2 \rightarrow YX_1$ *analytically* without any kinematical complications caused by boosts or rotations is the X_2RF , (often difficult or sometimes impossible to reconstruct event by event). As a result, there exists a subtle mismatch between the transparent theoretical description in the X_2RF and the direct experimental determination of spins and dynamical properties in the LAB . As worked out in detail later, the quantum state and polarization of the particle Y in the LAB are related to those in the X_2RF by several well-established kinematical functions which fully encode the impact of the *Wick helicity rotation* [34], (closely related but

¹Generally, azimuthal-angle correlations can be included in the analysis as well, but they involve quantum interference among the states with different helicities and require by far more complicated kinematic reconstructions [28]. For the sake of simple and straightforward kinematical analyses, we do not consider them here, postponing the analysis involving azimuthal-angle correlations as our later project.

²In principle any multi-body decay modes of the particle Y can be considered for extracting the information on Y polarization.

not identical to the Wigner rotation [1]) that is induced from two consecutive non-parallel Lorentz transformations.

The polarization parameters of Y in the X_2 RF are given *simply* by dynamical parameters such as spins, couplings, mixing matrices and masses of the particles involved in the two-body decay. On the contrary, the polarization parameters of Y in the LAB are connected *directly* to the sequential decay(s) of Y so that they can be measured and determined directly in experiments as they often do not require the full kinematic reconstruction of the entire event chain.

One transparent path for connecting the values of polarization parameters measured experimentally in the LAB with the dynamical theory parameters encoded in the X_2 decay amplitudes is provided by the helicity formalism [35–37], allowing us to deal with massless and massive particles on an equal footing. Without any specific assumptions on particle spins and masses, we provide a general spin analysis for predicting the LAB values of the polarization parameters and comparing them directly through angular correlations. In order to cover the case when the Y_2 polar-angle is not determined event by event, we integrate the correlations over the Y polar angle so as to derive the single polar-angle distribution of one of the Y decay products. The single polar-angle distribution can be expressed in terms of two polarization estimator functions (PEFs) for unpolarized X_2 particles [38–41] and eight polarization estimator functions appearing with non-zero X_2 polarization and accompanied by explicit trigonometric functions of the Y polar angle θ if the spin values are restricted up to one, i.e. 0, 1/2 and 1. All of the PEFs are functions in the X_2 speed β_2 in the LAB and the Y speed β in the X_2 RF fixed with the $X_{1,2}$ and Y masses, $m_{1,2}$ and m .

This paper consists of six main sections and three appendices. After this introduction part, Section 2 gives a general description of the construction of a helicity state of a particle and the transformation of its related helicity amplitudes by Wick helicity rotation. Once we derive the Y -helicity dependent polar-angle distribution in the X_2 RF by integrating the angle-dependent distribution over the Y azimuthal angle, then we can employ a proper Wick helicity rotation to get the polar-angle distribution depending directly on the Y helicities in the LAB. This final angular distribution to be called a Wick helicity rotation distribution function (WDF) involves only the diagonal elements of the X_2 polarization density matrix after an azimuthal-angle integration and this can be *directly* coupled to any polarized decay distribution of the particle Y . In order to facilitate the derivation of WDFs we introduce so-called Wick helicity rotation spectral functions (WSFs) solely consisting of the pure kinematic elements for the Wick helicity rotation and the explicitly angle-dependent part of the helicity amplitude in the X_2 RF, which plays a key role in connecting the X_2 polarization to the dynamical structure encoded in the reduced helicity amplitudes and for generating the Y polarization density matrix. Section 3 is devoted to combining the Y density matrix encoding the polarization-dependent angular distributions of the decay $X_2 \rightarrow YX_1$ with the sequential decay $Y \rightarrow ab$ into a correlation function of two polar angles, the Y polar-angle θ in the X_2 RF and the a polar-angle θ_a , in the Y rest frame. In Section 4 we introduce polarization estimator functions to be used for expressing the single polar-angle correlation derived by integrating the polar-angle correlation over the Y polar angle so as to cover the situation when the Y polar-angle with respect to the X_2 flight direction cannot be measured experimentally.

In Section 5 we demonstrate the formalism for polar-angle correlations explicitly by studying two SM examples, the sequential process $e^-e^+ \rightarrow Z \rightarrow \tau^-\tau^+ \rightarrow (\rho^-\nu_\tau)\tau^+ \rightarrow ([\pi^-\pi^0]\nu_\tau)\tau^+$ treating τ^+ inclusively, the sequential process $e^-e^+ \rightarrow t\bar{t} \rightarrow (W^+b)\bar{t} \rightarrow ([\ell^+\nu_\ell]b)\bar{t}$, treating \bar{t} inclusively, and one example in a model beyond the SM with a heavy vector-like top quark, $T \rightarrow Zt \rightarrow [\ell^-\ell^+]t$, as one of the characteristic non-standard examples. Section 6 contains a summary of our results and concluding remarks. After that, three appendices collecting a lot of mathematical formulas to be used in the main text are added. Appendix A is for introducing Wigner d -functions and listing a few properties to be exploited in the present work. Appendix B lists all the WDFs and the Y polarization density matrices in the general form so that they can be applied to any specific two-stage decays with no further refinements. Finally, we present the explicit forms of

all the non-trivial polarization estimator functions and investigate their asymptotic behaviors in Appendix C.

2 Wick helicity rotation on helicity states and helicity amplitudes

A helicity state $|p, j\lambda\rangle$ of a single spin- j particle with helicity λ and its four-momentum $p = (E, \vec{p}) = E(1, \beta \sin \theta \cos \phi, \beta \sin \theta \sin \phi, \beta \cos \theta)$ satisfying $\beta = |\vec{p}|/E = \sqrt{1 - m^2/E^2}$ in a given reference frame is defined by applying a sequence of boost and rotation transformations to a spin- j angular-momentum eigenstate $|j\lambda\rangle$ with the z -axis spin component λ in the rest frame with a fixed coordinate system as [4, 36]

$$|p, j\lambda\rangle = R_z(\phi)R_y(\theta)L_z(\beta)|j\lambda\rangle, \quad (3)$$

where the combined operation $R_z(\phi)R_y(\theta) = R(\phi, \theta, 0)$ is a rotation³ taking the z -axis into the direction of \vec{p} with spherical angles $\Omega = (\theta, \phi)$ and $L_z(\beta)$ is a pure boost along the z -axis direction from the rest frame to the frame where the particle speed is β . In contrast, the pure Lorentz transformation by a boost vector $\vec{\beta}$ preserving the assigned coordinate system is $L(\vec{\beta}) = R(\phi, \theta, 0)L_z(\beta)R^{-1}(\phi, \theta, 0)$. For convenience we define the sequence of operations on the right-hand side in Eq. (3) as an operation $h(\vec{\beta})$:

$$h(\vec{\beta}) = R_z(\phi)R_y(\theta)L_z(\beta) = L(\vec{\beta})R(\phi, \theta, 0), \quad (4)$$

with $\vec{\beta} = \vec{p}/E$. By definition, the helicity quantum number λ is the component of the spin along the momentum \vec{p} and it is a rotationally-invariant quantity.

The general theoretical analysis of the polarization of the particle Y of spin j in the two-body decay $X_2 \rightarrow Y X_1$ is most transparent in the X_2 RF frame if performed in the helicity formalism [36]. The decay helicity amplitude can be decomposed in terms of the decay polar and azimuthal angles for the momentum direction of the particle Y produced in the X_2 RF as

$$D_{\sigma_2: \sigma \sigma_1}^R(\theta, \phi) = F_{\sigma \sigma_1}^{j_2} d_{\sigma_2, \sigma - \sigma_1}^{j_2}(\theta) e^{i\sigma_2 \phi} \quad \text{with} \quad |\sigma - \sigma_1| \leq j_2, \quad (5)$$

where j_2 and σ_2 are the spin and helicity of the particle X_2 , and σ and σ_1 are the helicities of the particles, Y and X_1 boson, respectively. For the sake of discussion the Y momentum direction will be referred to as the production axis in the following. Because of rotational invariance, the reduced matrix elements $F_{\sigma \sigma_1}^{j_2}$ in Eq. (5) containing all the dynamical information on the decay process is independent of the X_2 helicity σ_2 .

The energy E and speed β of the particle Y in the decay $X_2 \rightarrow Y X_1$ are fixed in the X_2 RF with the masses $\{m_2, m, m_1\}$ of the three particles as

$$E = \frac{m_2^2 - m_1^2 + m^2}{2m_2} \quad \text{and} \quad \beta = \frac{\lambda^{1/2}(m_2^2, m_1^2, m^2)}{m_2^2 - m_1^2 + m^2}, \quad (6)$$

with the magnitude of momentum $|\vec{p}| = \beta E$ and the Källén kinematical function $\lambda(x, y, z) = x^2 + y^2 + z^2 - 2xy - 2yz - 2zx = (x - y - z)^2 - 4yz$ [42].

The polarizations of the particle Y determined with respect to the detection axis of the Y momentum direction in the LAB is related to those in the X_2 RF frame by a Wick helicity rotation connecting the two helicity bases [34]. The Wick helicity rotation angle ω is determined by taking the three sequential operations consisting of the Lorentz transformation $h_{2Y}(\vec{\beta})$ from the YRF to X_2 RF, followed by the pure

³It should be noted that this rotation is simpler than the one introduced in the original paper by Jacob and Wick corresponding to $R(\phi, \theta, -\phi)$ in Ref. [35].

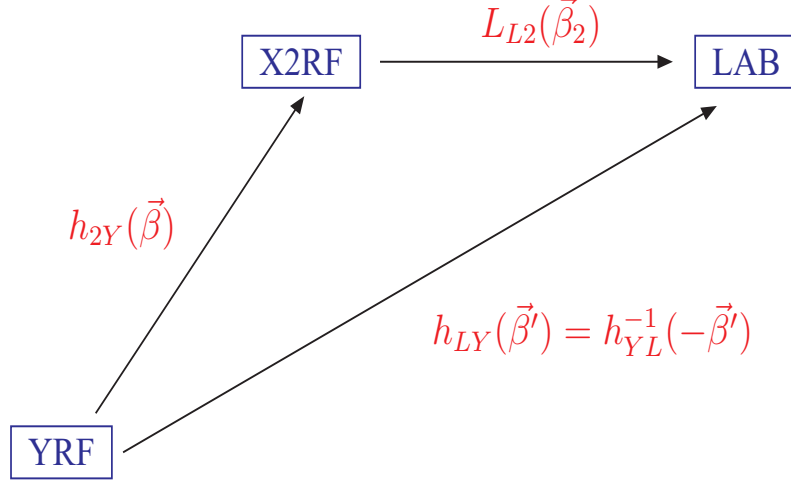


Figure 1: A simple diagrammatic description of the Wick helicity rotation describing the mismatch between the two helicity coordinate systems of the LAB directly reached through one single Lorentz transformation $h_{LY}(\vec{\beta}_2) = \Lambda_{YL}^{-1}(-\vec{\beta}_2)$ and indirectly reached through the Lorentz transformation $h_{2Y}(\vec{\beta})$ from the rest frame of Y (YRF) to the X_2 RF and then the pure coordinate-preserving Lorentz transformation $L_{L2}(\vec{\beta}_2)$ from the X_2 RF to the LAB, from the YRF. The boost parameter β_2 is the X_2 speed in the LAB and the parameters, β and β' , are the speed of the particle Y in the X_2 RF and LAB, respectively.

coordinate-preserving Lorentz transformation $L_{L2}(\vec{\beta}_2)$ from the X_2 RF frame to the LAB, and finally the Lorentz transformation $h_{YL}(-\vec{\beta}') = h_{LY}^{-1}(\vec{\beta}')$ transforming back the system from the LAB to the YRF as

$$\mathcal{R}(\vec{\omega}) = h_{LY}^{-1}(\vec{\beta}') L_{L2}(\vec{\beta}_2) h_{2Y}(\vec{\beta}) = h_{YL}(-\vec{\beta}') L_{L2}(\vec{\beta}_2) h_{2Y}(\vec{\beta}), \quad (7)$$

with the $\vec{\omega}$ direction parallel to $\vec{\beta}_2 \times \vec{\beta}$, where h , L , and \mathcal{R} are the representation matrices for the Lorentz transformations. A simple diagrammatic description for the Wick helicity rotation is shown in Fig. 1. Explicitly, the Y velocity $\vec{\beta}'$ in the LAB is related to the Y velocity $\vec{\beta}$ in the X_2 RF by

$$\vec{\beta}' = \frac{1}{\gamma_2 (1 + \vec{\beta}_2 \cdot \vec{\beta})} \left[\vec{\beta} + \gamma_2 \vec{\beta}_2 + \frac{\gamma_2^2}{\gamma_2 + 1} (\vec{\beta}_2 \cdot \vec{\beta}) \vec{\beta}_2 \right] = \frac{\gamma_2^{-1} \vec{\beta}_\perp + \vec{\beta}_\parallel + \vec{\beta}_2}{1 + \vec{\beta}_2 \cdot \vec{\beta}}, \quad (8)$$

in terms of the velocities, $\vec{\beta}$ and $\vec{\beta}_2$, with $\gamma_2 = 1/\sqrt{1 - \beta_2^2}$, and the Wick helicity rotation angle ω defined by the relation in Eq. (7) can be extracted from the expressions of the standard tangent function

$$\tan \omega = \frac{\beta_2 \sqrt{1 - \beta^2} \sin \theta}{\beta + \beta_2 \cos \theta}, \quad (9)$$

and/or those of the sine and cosine functions

$$\sin \omega = \frac{\beta_2 \sqrt{1 - \beta^2} \sin \theta}{\sqrt{(\beta_2 \beta \cos \theta + 1)^2 - (1 - \beta_2^2)(1 - \beta^2)}}, \quad (10)$$

$$\cos \omega = \frac{\beta + \beta_2 \cos \theta}{\sqrt{(\beta_2 \beta \cos \theta + 1)^2 - (1 - \beta_2^2)(1 - \beta^2)}}, \quad (11)$$

in terms of the Y speed and polar angle, β and θ , in the X_2 RF and the X_2 speed, β_2 , in the LAB. Similarly, the angle ω_1 of the Wick helicity rotation for the X_1 helicity state and distributions in the LAB can be

obtained from Eq. (9) by replacing θ by $\pi - \theta$ and β by β_1 , the X_1 speed in the X_2 RF.

There are two extreme kinematic limits for which we do not have to rely on any detailed information on the boost distributions in practice. Firstly, if the particle X_2 is produced near threshold with $\beta_2 \rightarrow 0$, then $\omega \rightarrow 0$ rendering the difference between the production and detection axes negligible. Secondly, if the mass splitting, $m_2 - m_1$, of the particles X_2 and X_1 is much larger than m , the particle Y is highly boosted with E and p much larger than m even in the X_2 rest frame except for the far backward region with θ very close to π . Naturally, $\omega = 0$ if the particle Y is massless, i.e. $\beta = 1$.

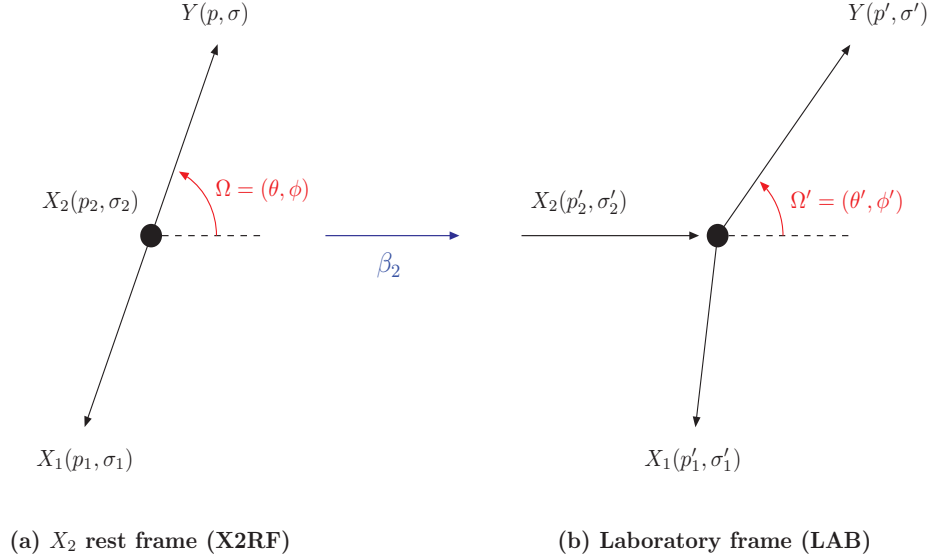


Figure 2: Kinematic configurations of the two-body decay $X_2 \rightarrow Y X_1$ in (a) the X_2 RF with $p_2 = (m_2, \vec{0})$ and (b) in the LAB. The unprimed (p_2, q, p_1) and $(\sigma_2, \sigma, \sigma_1)$ are the momenta and helicities of the X_2, Y and X_1 particles in the X_2 RF while the corresponding primed momenta and helicities are defined in the LAB. The solid angles, $\Omega = (\theta, \phi)$ and $\Omega' = (\theta', \phi')$, which are defined with respect to the X_2 momentum direction in the LAB, are the polar and azimuthal angles of the particle Y in the X_2 RF and in the LAB, respectively. The boost parameter β_2 , which links the X_2 RF and LAB, is nothing but the X_2 speed in the LAB. Note that the azimuthal angles of the particle Y and the X_2 helicities are identical, i.e. $\phi' = \phi$ and $\sigma'_2 = \sigma_2$ for the boost.

Let us consider a fixed 3-dimensional spatial coordinate system of the X_2 RF with the positive z -axis along the X_2 momentum direction $\vec{\beta}_2$ in the LAB. In this situation the X_2 helicity is invariant under the boost along the X_2 momentum direction from the X_2 RF to the LAB so that the helicity states of the particles, Y and X_1 , in the LAB are given in terms of the corresponding helicity states in the X_2 RF by

$$|p', j\sigma'\rangle = \sum_{\sigma} d_{\sigma', \sigma}^j(\omega) |p, j\sigma\rangle \quad \text{and} \quad |p'_1, j_1\sigma'_1\rangle = \sum_{\sigma_1} d_{\sigma'_1, \sigma_1}^{j_1}(\omega_1) |p_1, j_1\sigma_1\rangle. \quad (12)$$

As a consequence, the decay helicity amplitudes in the LAB for the two-body decay are related to those in the X_2 RF through two Wick helicity rotations on the Y and X_1 states as

$$D_{\sigma'_2, \sigma', \sigma'_1}^L(\theta', \phi') = \sum_{\sigma, \sigma_1} d_{\sigma', \sigma}^j(\omega) d_{\sigma'_1, \sigma_1}^{j_1}(\omega_1) D_{\sigma'_2, \sigma, \sigma_1}^R(\theta, \phi), \quad (13)$$

with $\phi' = \phi$ of the particle Y for this specific Lorentz boost $L_{L2}(\beta_2 \hat{z})$. The polar angle θ' and the energy E' of Y particle in the LAB are expressed in terms of to the polar angle θ as

$$\tan \theta' = \frac{\beta \sin \theta}{\gamma_2(\beta_2 + \beta \cos \theta)} \quad \text{and} \quad E' = \gamma_2(1 + \beta_2 \beta \cos \theta) E, \quad (14)$$

with the explicit forms of E and β in Eq. (6). It is noteworthy that, if neither β_2 nor β is zero, the polar-angle distribution in the X_2 RF can be derived directly from the Y energy distribution in the LAB. The kinematic configurations of the two-body decay $X_2 \rightarrow YX_1$ in the X_2 RF and LAB are displayed in Fig. 2.

In order to describe the impact of the X_2 polarization on the Y polarization and angular distribution in the LAB in a general footing, we introduce the $(2j_2 + 1) \times (2j_2 + 1)$ helicity density matrix ρ^{X_2} containing the full information on the X_2 polarization and satisfying the normalization condition $\text{Tr}(\rho^{X_2}) = 1$. Integrating over the azimuthal angle ϕ we can obtain the helicity-dependent distribution in the X_2 RF as

$$\mathcal{D}_{\sigma\lambda}(\theta) = \sum_{\sigma_2} \sum_{\sigma_1} \rho_{\sigma_2, \sigma_2}^{X_2} [d_{\sigma_2, \sigma - \sigma_1}^{j_2}(\theta) d_{\sigma_2, \lambda - \sigma_1}^{j_2}(\theta)] F_{\sigma\sigma_1}^{j_2} F_{\lambda\sigma_1}^{j_2*}. \quad (15)$$

By performing the integration⁴ over the azimuthal angle ϕ' , which is identical to ϕ under the Lorentz transformation $L_{L2}(\beta_2 \hat{z})$, and taking the sum over the X_1 helicity σ'_1 , we can obtain a fully-correlated and Wick-rotated distribution, from which the $(2j + 1) \times (2j + 1)$ polarization density matrix of the particle Y in the LAB can be derived, as

$$\mathcal{D}'_{\sigma'\lambda'}(\omega, \theta) = \sum_{\sigma, \lambda} [d_{\sigma', \sigma}^j(\omega) d_{\lambda', \lambda}^j(\omega)] \mathcal{D}_{\sigma\lambda}(\theta), \quad (16)$$

$$= \sum_{\sigma_2} \sum_{\sigma, \lambda} \sum_{\sigma_1} \rho_{\sigma_2, \sigma_2}^{X_2} [d_{\sigma', \sigma}^j(\omega) d_{\lambda', \lambda}^j(\omega)] [d_{\sigma_2, \sigma - \sigma_1}^{j_2}(\theta) d_{\sigma_2, \lambda - \sigma_1}^{j_2}(\theta)] F_{\sigma\sigma_1}^{j_2} F_{\lambda\sigma_1}^{j_2*}, \quad (17)$$

to be called *Wick helicity rotation distribution functions (WDFs)* involving only the diagonal components of the density matrix ρ^{X_2} , where the general form in Eq. (5) of the two-body decay helicity amplitude has been taken into account. The polar-angle and polarization dependent decay width is then given by

$$\frac{d\Gamma_{\sigma'\lambda'}}{d \cos \theta} = \gamma_2 \beta_2 \beta E \frac{d\Gamma_{\sigma'\lambda'}}{dE'} = \frac{\bar{\beta}}{16\pi\gamma_2 m_2} \mathcal{D}'_{\sigma'\lambda'}(\omega, \theta), \quad (18)$$

where the boost factor $\gamma_2 = 1/\sqrt{1 - \beta_2^2}$ and the abbreviation $\bar{\beta} = \lambda^{1/2}(1, m_1^2/m_2^2, m^2/m_2^2)$. For the sake of our discussion, we cast the expression of WDFs in Eq. (17) into a little shorter form:

$$\mathcal{D}'_{\sigma'\lambda'}(\omega, \theta) = \sum_{\sigma_2} \sum_{\sigma, \lambda} \sum_{\sigma_1} \rho_{\sigma_2, \sigma_2}^{X_2} \times \mathcal{S}_{\sigma_2; \sigma'\lambda'}^{\sigma\lambda; \sigma_1}(\omega, \theta) \times F_{\sigma\sigma_1}^{j_2} F_{\lambda\sigma_1}^{j_2*}, \quad (19)$$

by introducing the following helicity and polar-angle dependent functions to be called *Wick helicity rotation spectral functions (WSFs)* as

$$\mathcal{S}_{\sigma_2; \sigma'\lambda'}^{\sigma\lambda; \sigma_1}(\omega, \theta) = [d_{\sigma', \sigma}^j(\omega) d_{\lambda', \lambda}^j(\omega)] \times [d_{\sigma_2, \sigma - \sigma_1}^{j_2}(\theta) d_{\sigma_2, \lambda - \sigma_1}^{j_2}(\theta)] \quad (20)$$

The averages of WSFs over the polar-angle θ to be named *Wick helicity rotation spectral elements (WSEs)* is given by

$$\langle \mathcal{S}_{\sigma_2; \sigma'\lambda'}^{\sigma\lambda; \sigma_1} \rangle = \frac{1}{2} \int_{-1}^1 \mathcal{S}_{\sigma_2; \sigma'\lambda'}^{\sigma\lambda; \sigma_1}(\omega, \theta) d \cos \theta. \quad (21)$$

⁴Even if the azimuthal angle distributions allow us to make a more detailed spin and angular-correlation analysis, we focus on the polar-angle distributions, while postponing the full correlations as our next project.

The WSFs satisfy the normalization conditions

$$\text{Tr}(S_{\sigma_2}^{\sigma\lambda;\sigma_1}) \equiv \sum_{\sigma'} S_{\sigma_2;\sigma'\sigma'}^{\sigma\lambda;\sigma_1} = \delta_{\sigma\lambda} [d_{\sigma_2,\sigma-\sigma_1}^{j_2}(\theta)]^2, \quad (22)$$

with no Wick helicity rotation effects, leading to a simple normalization for the WSEs as

$$\text{Tr}(\langle S_{\sigma_2}^{\sigma\lambda;\sigma_1} \rangle) \equiv \sum_{\sigma'} \langle S_{\sigma_2;\sigma'\sigma'}^{\sigma\lambda;\sigma_1} \rangle = \begin{cases} \delta_{\sigma\lambda}/(2j_2 + 1) & \text{if } |\sigma - \sigma_1| \leq j_2, \\ 0 & \text{if } |\sigma - \sigma_1| > j_2, \end{cases} \quad (23)$$

that is independent of the X_2 helicity σ_2 .

The normalized polar-angle dependent distribution W' and the integrated polarization density matrix ρ^Y of the particle Y are obtained from the WDFs in Eq. (17) as

$$W'_{\sigma'\lambda'}(\theta) = \frac{\mathcal{D}'_{\sigma'\lambda'}(\omega, \theta)}{\text{Tr}[\langle \mathcal{D}' \rangle]} \quad \text{and} \quad \rho_{\sigma'\lambda'}^Y = \frac{\langle \mathcal{D}'_{\sigma'\lambda'}(\omega, \theta) \rangle}{\text{Tr}[\langle \mathcal{D}' \rangle]}, \quad (24)$$

satisfying the normalization conditions, $\text{Tr}[\langle W' \rangle] = 1$ and $\text{Tr}(\rho^Y) = 1$. They will be combined later with the polarized Y decay distributions, for correlated polar-angle distributions and single polar-angle distributions. The explicit expressions of the matrix elements will be presented in detail for a specific set of decay processes later in Section 5 and the polarization density matrices ρ^Y are listed in their general form for the cases with particle spins up to one in Appendix B.

In passing we note that the partial decay width $\Gamma[X_2 \rightarrow YX_1]_{LAB}$ in the LAB is obtained by summing up the diagonal elements of the distribution matrix in Eq. (17) over the Y helicity σ' and integrating it over the polar angle θ as

$$\Gamma[X_2 \rightarrow YX_1]_{LAB} = \frac{1}{\gamma_2} \Gamma[X_2 \rightarrow YX_1] = \frac{\bar{\beta}}{8\pi\gamma_2 m_2} \frac{1}{(2j_2 + 1)} \sum'_{\sigma, \sigma_1} |F_{\sigma\sigma_1}^{j_1}|^2, \quad (25)$$

with the boost factor γ_2 of the particle X_2 of speed β_2 in the LAB, reflecting time dilation. The prime on the summation notation indicates that the sum is taken only when $|\sigma - \sigma_1| \leq j_2$ is satisfied.

3 Polar-angle correlations and their reconstruction

Extracting efficiently the essential information on the X_2 polarization and the dynamics of the two-body decay $X_2 \rightarrow YX_1$ encoded in the Y density matrix $\rho^Y(\theta)$ in Eq. (24) require exploiting Y -polarization sensitive decays.

With no serious loss of generality, we assume that Y decays into two particles, a particle a of mass m_a and spin j_a and a particle b of mass m_b and spin j_b of which the helicity amplitude can be written in the Y rest frame as

$$D_{\sigma;\sigma_a\sigma_b}(\theta_a, \phi_a) = H_{\sigma_a\sigma_b}^j d_{\sigma,\sigma_a-\sigma_b}^j(\theta_a) e^{i\sigma\phi_a}, \quad (26)$$

where the polar and azimuthal angles θ_a and ϕ_a define the momentum direction of the particle a in a coordinate system with the positive z axis along the Y flight direction in the LAB.

After combining the Y production and decay amplitudes and integrating the combined distribution over the azimuthal angle ϕ_a , we obtain a correlated distribution of two polar angles, θ and θ_a , as

$$\frac{d^2\mathcal{C}}{d\cos\theta d\cos\theta_a} = \frac{(2j+1)}{4} \sum_{\sigma'=-j}^j W'_{\sigma'\sigma'}(\theta) \rho_{\sigma'\sigma'}^D(\theta_a), \quad (27)$$

with the Y decay density matrix ρ^Y defined in terms of the decay helicity amplitudes as

$$\rho_{\sigma'\sigma}^D(\theta_a) = \frac{\sum_{\sigma_a\sigma_b} [d_{\sigma',\sigma_a-\sigma_b}^j(\theta_a)]^2 |H_{\sigma_a\sigma_b}^j|^2}{\sum_{\sigma_a\sigma_b} |H_{\sigma_a\sigma_b}^j|^2}, \quad (28)$$

The polar-angle correlation in Eq. (27) encodes the full information on the dynamics of the two-stage decay $X_2 \rightarrow YX_1 \rightarrow (ab)X_1$ that can be extracted through measuring the polar angles, θ and θ_a , experimentally. Here, we emphasize that the correlation function depends also on the X_2 speed β_2 as well. In the following analysis, we assume that the speed β_2 is determined event by event or the β_2 -dependent distribution is known already so that it can be folded with the correlation function for a full-fledged distribution.

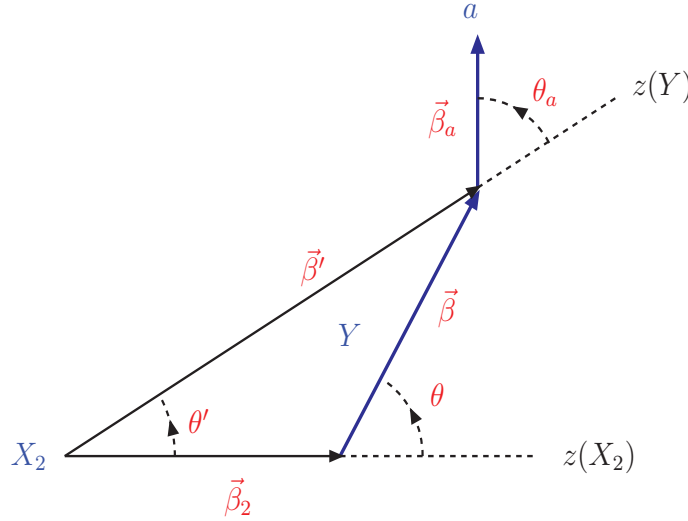


Figure 3: A simple diagram describing the relation among the polar angles, θ in the X_2 RF and θ' in the LAB, and the polar angle θ_a of the particle in the Y rest frame from the decay $Y \rightarrow a + b$. $\vec{\beta}_2$ is the X_2 velocity in the LAB and $\vec{\beta}$ ($\vec{\beta}'$) and θ (θ') are the Y velocity and polar angle in the X_2 RF (LAB). Also, $\vec{\beta}_a$ and θ_a are the a velocity and polar angle in the Y RF. $z(X_2)$ and $z(Y)$ denote the X_2 and Y flight directions in the LAB. Note that the relative orientation between the plane formed by $\vec{\beta}_2$ and $\vec{\beta}$ and the plane formed by $\vec{\beta}'$ and $\vec{\beta}_1$ can be arbitrary. In this light, all the azimuthal angles are not displayed for simplicity, because they are irrelevant to the polar-angle correlations under our considerations.

The most straightforward way of determining the polar angles θ and θ_a is through the measurement of

the Y and a energies, E' and E'_a , in the LAB, as they satisfy the relations:

$$\cos \theta = \frac{1}{\gamma_2 \beta_2 \gamma \beta} \left[\frac{E'}{m} - \gamma_2 \gamma \right], \quad (29)$$

$$\cos \theta_a = \frac{1}{\gamma' \beta' \gamma_a \beta_a} \left[\frac{E'_a}{m_a} - \gamma' \gamma_a \right], \quad (30)$$

where the Y boost factors, γ' and β' , in the LAB are given in terms of the X_2 boost factors in the LAB, β_2 and γ_2 , and the Y polar angle θ and Y boost factors γ and β in the X_2 RF by

$$\gamma' = \frac{E'}{m} = \gamma_2 \gamma (1 + \beta_2 \beta \cos \theta) \quad \text{and} \quad \beta' = \sqrt{1 - 1/\gamma'^2}, \quad (31)$$

as can be checked with Eq. (29). The value of γ' varies between $\gamma_2 \gamma (1 - \beta_2 \beta \cos \theta)$ and $\gamma_2 \gamma (1 + \beta_2 \beta \cos \theta)$ and, for a given value of γ' , the allowed range of the a boost factor $\gamma'_a = E'_a/m_a$ is between $\gamma'_{a\min} = \gamma' \gamma_a (1 - \beta' \beta_a)$ and $\gamma'_{a\max} = \gamma' \gamma_a (1 + \beta' \beta_a)$ with $\gamma_a = (m^2 + m_a^2 - m_b^2)/2mm_a$. A simple diagrammatic description of the kinematic relations among angles and boost parameters is shown in Fig. 3. Note that $\vec{\beta}'$ is not a simple vector sum of $\vec{\beta}_2$ and $\vec{\beta}$ but a complicated combination of them as shown in Eq. (8).

If the polar angle θ in the X_2 RF cannot be measured but the four-momentum of Y or one of the Y decay products can be fully reconstructed, then we can still use the one-dimensional θ_a distribution derived by integrating the 2-dimensional distribution in Eq. (27) over the polar angle θ . In general there are thirteen independent functions of the Wick angle ω and θ to be integrated over the angle θ . Three of them are rather trivial as they depend simply on θ . The remaining ten integrated functions, which we call polarization estimator functions (PEFs), will be classified and described in detail in the next section, while their expressions with spins up to one are listed in Appendix C.

4 Polarization estimator functions

If the spin of the particle Y is $j = 0$, there are no Wick helicity rotation effects and so the production-decay correlation distribution of the particle X_2 is simply given by the θ -dependent function

$$\mathcal{D}'(\omega, \theta) = \mathcal{D}'(0, \theta) = \sum_{\sigma_2} \sum_{\sigma_1}' \rho_{\sigma_2, \sigma_2}^{X_2} \left[d_{\sigma_2, -\sigma_1}^{j_2}(\theta) \right]^2 |F_{\sigma_1}^{j_2}|^2, \quad (32)$$

with the restriction $|\sigma_1'| \leq j_2$. Furthermore, for a spin-0 particle X_2 the helicity density matrix ρ^{X_2} is trivially one, resulting in no production-decay correlations at all.

On the contrary, non-trivial Wick helicity rotation effects are developed for non-zero Y spins. Although the formalism given in Section 2 can be applied to any spin combination, we consider the cases with spin values, 0, 1/2 and 1 for showing the *diagonal* correlated distributions ($\sigma' = \lambda'$) - WDFs and WSFs explicitly in the present work as they are directly related with the sequential polar-angle decay distributions of the particle Y after azimuthal-angle integration.

Applying the coupling rule of Wigner d -functions in Eq. (A.14) we can rewrite the diagonal WDFs $\mathcal{D}_{\sigma'\sigma'}$ in the form as

$$\mathcal{D}'_{\sigma'\sigma'}(\omega, \theta) = \sum_{J=0}^{2j} \sum_{J_2=0}^{2j_2} \sum_{\sigma, \lambda=-j}^j C_{\sigma\lambda; \sigma'}^{JJ_2} [d_{0, \sigma-\lambda}^J(\omega) d_{0, \sigma-\lambda}^{J_2}(\theta)], \quad (33)$$

where the coefficients $C_{\sigma\lambda;\sigma'}^{JJ_2}$ are determined by a combination of the elements of the density matrix ρ^{X_2} , the reduced decay helicity amplitudes $F_{\sigma\sigma_1}^{j_2}$ and $F_{\lambda\sigma_1}^{j_2^*}$ and four Clebsch-Gordan coefficients. The general form of $d_{0\lambda}^J(\beta)$ expressed in terms of the standard Legendre polynomial $P_J(\cos\beta)$ by the formula [43]

$$d_{0\lambda}^J(\beta) = 2^\lambda \left(\frac{\cos\beta}{2}\right)^\lambda \left(\frac{\sin\beta}{2}\right)^\lambda \sqrt{\frac{(J-\lambda)!}{(J+\lambda)!}} \frac{d^\lambda}{d\cos\beta^\lambda} P_J(\cos\beta), \quad (34)$$

for integral J and λ . Taking into account the expressions of six $d_{0\lambda}^J$ functions up to $J = 2$ with $\lambda \geq 0$:

$$d_{00}^0(\beta) = 1; \quad d_{00}^1(\beta) = \cos\beta, \quad d_{01}^1(\beta) = \frac{\sin\beta}{\sqrt{2}}; \quad (35)$$

$$d_{00}^2(\beta) = \frac{1}{2}(3\cos^2\beta - 1), \quad d_{01}^2(\beta) = \sqrt{\frac{3}{2}}\cos\beta\sin\beta, \quad d_{02}^2(\beta) = \sqrt{\frac{3}{8}}(1 - \cos^2\beta), \quad (36)$$

and three additional d -functions with negative λ values derived with the relation $d_{0\lambda}^J(\beta) = (-1)^\lambda d_{0,-\lambda}^J$, ten non-trivial β_2 and β dependent polarization estimator functions (PEFs) can be formed:

$$\begin{aligned} \langle \cos\omega \rangle, & \quad \langle \cos\omega \cos\theta \rangle, & \quad \langle \cos\omega \cos 2\theta \rangle, \\ \langle \cos^2\omega \rangle, & \quad \langle \cos^2\omega \cos\theta \rangle, & \quad \langle \cos^2\omega \cos^2\theta \rangle, \\ & \quad \langle \sin\omega \sin\theta \rangle, & \quad \langle \sin\omega \sin 2\theta \rangle, \\ & \quad \langle \cos\omega \sin\omega \sin\theta \rangle, & \quad \langle \cos\omega \sin\omega \cos\theta \sin\theta \rangle, \end{aligned} \quad (37)$$

where the bracket stands for the average over the polar-angle θ defined as

$$\langle F(\omega, \theta) \rangle = \frac{1}{2} \int_{-1}^1 F(\omega, \theta) d\cos\theta, \quad (38)$$

for any function $F(\omega, \theta)$ dependent on θ implicitly as well as explicitly.⁵ Two PEFs, $\langle \cos\omega \rangle$ and $\langle \cos^2\omega \rangle$ with no explicit θ -dependence, were already introduced in Refs. [38–41], which appear even in the case of unpolarized X_2 . The detailed expressions and the properties of all the ten non-trivial polarization estimator functions are listed and described in detail in Appendix C.

Table 1 shows all the non-trivial PEFs that may contribute to the polar-angle averages of WDFs in the decay process with the spin combinations of $j_2 \rightarrow j + j_1$ involving all the spin values up to one. The notation $\|jj_1\|$ stands for the final state with Y of spin j and X_1 of spin j_1 . The symbol \bullet indicates the polarization estimator functions may show up in the corresponding decay mode, but the symbol \surd implies that the corresponding PEF can appear only when parity is violated in the two-body decay.

5 Examples of the Wick helicity rotation in the Standard Model and beyond

Spin has played a dramatic role in the field of elementary particle physics, acting as a powerful tool in the confirmation and verification of particle physics theories, especially in numerous tests of the SM since its birth about fifty years ago [44–47]. In this section, we apply the formalism developed in the previous sections to two well-known SM cases and one non-standard case with a new heavy vectorlike top quark, eventually deriving the two-stage polar-angle correlations in their full form. On the other hand, we present a few simple numerical analyses while postponing more comprehensive numerical studies as a next project.

⁵As can be checked with Eq. (33), every $\sin\omega$ due to the interference of two Y states of different helicities in the X_2 RF is always accompanied by $\sin\theta$ so that $\langle \sin\omega \rangle$ and $\langle \cos\omega \sin\omega \rangle$ cannot show up.

Polarization Estimator Functions

X_s spin	$j_2 = 0$			$j_2 = \frac{1}{2}$			$j_2 = 1$		
$Y \& X_1$ spins: $\ j j_1\ $	$\ \frac{1}{2} \frac{1}{2}\ $	$\ 10\ $	$\ 11\ $	$\ \frac{1}{2}0\ $	$\ \frac{1}{2}1\ $	$\ 1\frac{1}{2}\ $	$\ \frac{1}{2}\frac{1}{2}\ $	$\ 10\ $	$\ 11\ $
$\langle \cos \omega \rangle$	✓		✓	✓	✓	✓	✓	✓	✓
$\langle \cos^2 \omega \rangle$		•	•				•	•	•
$\langle \cos \omega \cos \theta \rangle$				•	•	•	•	•	•
$\langle \cos \omega \cos^2 \theta \rangle$							✓	✓	✓
$\langle \cos^2 \omega \cos \theta \rangle$						✓		✓	✓
$\langle \cos^2 \omega \cos^2 \theta \rangle$								•	•
$\langle \sin \omega \sin \theta \rangle$				•	•	•	•	•	•
$\langle \sin \omega \cos \theta \sin \theta \rangle$							✓	✓	✓
$\langle \cos \omega \sin \omega \sin \theta \rangle$						✓		✓	✓
$\langle \cos \omega \sin \omega \cos \theta \sin \theta \rangle$								•	•

Table 1: List of non-trivial polarization estimator functions which may contribute to the polar-angle averages of WDFs in the decay process $j_2 \rightarrow j + j_1$ involving all the spin values up to 1. The notation $\|j j_1\|$ stands for the final state with Y of spin j and X_1 of spin j_1 and the symbol • indicates the polarization estimator functions may show up in the corresponding decay mode, but the symbol ✓ implies that the corresponding PEF can appear only when parity is violated in the two-body decay. Note that every term involving an odd number of cosines can show up with parity-violating interactions.

5.1 The process $e^- e^+ \rightarrow Z \rightarrow \tau^- \tau^+$ followed by $\tau^- \rightarrow \rho^- \nu_\tau$ and $\rho^- \rightarrow \pi^- \pi^0$

As a characteristic example of the key decay mode with the spin combination of $1/2 \rightarrow 1 + 1/2$, we consider the following three-stage sequential processes of the SM, established with exquisite precision experimentally at SLAC and LEP and in the SM [48]:

$$e^- e^+ \rightarrow Z \rightarrow \tau^- \tau^+ \rightarrow (\rho^- \nu_\tau) \tau^+ \rightarrow ([\pi^- \pi^0] \nu_\tau) \tau^+, \quad (39)$$

where τ^+ is assumed to be inclusively measured. The key chain for our analysis in Eq. (39) is the two-body decay $\tau^- \rightarrow \rho^- \nu_\tau$, one of the main τ decay modes [49–54]. The τ -pair production process proceeds at the tree level through two s -channel γ and Z exchanges. On the Z -boson pole, the contribution from γ exchange is of order $\Gamma_Z/m_Z \sim 0.027$ compared with that of Z exchange [55] so that the γ -exchange contribution can be neglected with good approximation, although it can be included easily if necessary. The sequential process in Eq. (39) is then viewed as a typical physical process of resonance formation and decay.

The Feynman rules of the eeZ and $Z\tau\tau$ vertices consist of vector and axial-vector structures:

$$\langle Z | e^- e^+ \rangle^\mu = -ig_Z \gamma^\mu (v_e - a_e \gamma_5), \quad (40)$$

$$\langle \tau^- \tau^+ | Z_\mu \rangle = -ig_Z \gamma_\mu (v_\tau - a_\tau \gamma_5), \quad (41)$$

with $g_Z = e/c_W s_W$ and the abbreviations, $s_W = \sin \theta_W$ and $c_W = \cos \theta_W$, of the weak-mixing angle θ_W . In the SM, $v_e = v_\tau = s_W^2 - 1/4$ and $a_e = a_\tau = -1/4$. Apart from a function related to the energy-dependent Z propagator and an azimuthal-angle dependent phase as well as a common gauge coupling g_Z , the helicity amplitude of the $\tau^- \tau^+$ pair production in $e^- e^+$ collisions can be written in the form

$$T_{\sigma_e \bar{\sigma}_e; \sigma_\tau \bar{\sigma}_\tau}(\Theta) = P_{\sigma_e \bar{\sigma}_e} D_{\sigma_\tau \bar{\sigma}_\tau} d_{\sigma_e - \bar{\sigma}_e, \sigma_\tau - \bar{\sigma}_\tau}^1(\Theta). \quad (42)$$

The labels, $(\sigma_e, \bar{\sigma}_e)$ and $(\sigma_\tau, \bar{\sigma}_\tau)$, refer to the helicities of the relevant particles e^\mp and τ^\mp , and $P_{\sigma_e \bar{\sigma}_e}$ and $D_{\sigma_\tau \bar{\sigma}_\tau}$ measure the helicity amplitudes for $e^- e^+ \rightarrow Z$ and $Z \rightarrow \tau^- \tau^+$, respectively.

If the electron mass m_e is neglected, then the electron and positron must have opposite helicity, yielding two surviving $e^- e^+ \rightarrow Z$ helicity amplitudes as

$$P_{\pm\mp} = v_e \mp a_e \quad \text{and} \quad P_{\pm\pm} = 0. \quad (43)$$

The latter vanishing result is due to chirality preservation in the limit of $m_e = 0$. On the other hand, with non-zero τ mass m_τ , the decay part consists of four helicity amplitudes

$$D_{\pm\mp} = v_\tau \mp \beta_\tau a_\tau, \quad (44)$$

$$D_{\pm\pm} = \frac{1}{\sqrt{2}} \sqrt{1 - \beta_\tau^2} v_\tau = \sqrt{2} \frac{m_\tau}{m_Z} v_\tau, \quad (45)$$

with the τ^- speed $\beta_\tau = \sqrt{1 - 4m_\tau^2/m_Z^2}$ in the $e^- e^+$ CM frame. Note that $\beta_\tau \simeq 1$ up to per-mille precision with $m_Z = 91$ GeV and $m_\tau = 1.78$ GeV on the Z -boson pole, i.e. the produced τ^\mp is highly relativistic.

For the sake of notation, we introduce two asymmetry parameters:

$$A_e = \frac{2v_e a_e}{v_e^2 + a_e^2} \quad \text{and} \quad A_\tau = \frac{2v_\tau a_\tau}{v_\tau^2 + a_\tau^2}, \quad (46)$$

and two polarization-dependent quantities

$$\xi_1 = -P_{e^-} P_{e^+} - A_e (P_{e^-} - P_{e^+}), \quad (47)$$

$$\xi_2 = -(P_{e^-} - P_{e^+}) - A_e P_{e^-} P_{e^+}. \quad (48)$$

Folding the e^- and e^+ diagonal 2×2 polarization density matrices $\rho_{e^\pm} = \frac{1}{2} \text{diag}(1 + P_{e^\pm}, 1 - P_{e^\pm})$ in the $(1/2, -1/2)$ helicity basis for longitudinally polarized electron and positron beams, with the squares of the transition amplitudes and then summing them over the τ^+ helicities we have the differential cross section given by

$$\frac{1}{\sigma_{unp}} \frac{d\sigma_{pol}}{d\cos\Theta} = \frac{3}{2} \frac{(1 + \xi_1)[1 + \cos^2\Theta + (1 - \beta_\tau^2)(\eta_\tau - \cos^2\Theta)] + 2(A_e + \xi_2) A_\tau \beta_\tau \cos\Theta}{3 + \beta_\tau^2 + 3\eta_\tau(1 - \beta_\tau^2)}, \quad (49)$$

with a ratio $\eta_\tau = (v_\tau^2 - a_\tau^2)/(v_\tau^2 + a_\tau^2)$ of the vector and axial-vector couplings in addition to A_e and A_τ .

The angular-dependent τ^- polarization $P_\tau(\Theta)$ in the $e^- e^+$ CM frame of a τ^- moving with speed β_τ and polar angle Θ reads

$$P_\tau(\Theta) = -\frac{(1 + \xi_1)A_\tau \beta_\tau (1 + \cos^2\Theta) + (A_e + \xi_2)[1 + \eta_\tau + (1 - \eta_\tau)\beta_\tau^2] \cos\Theta}{(1 + \xi_1)[1 + \cos^2\Theta + (1 - \beta_\tau^2)(\eta_\tau - \cos^2\Theta)] + 2(A_e + \xi_2)A_\tau \beta_\tau \cos\Theta}, \quad (50)$$

$$\Rightarrow -\frac{(1 + \xi_1)A_\tau (1 + \cos^2\Theta) + 2(A_e + \xi_2) \cos\Theta}{(1 + \xi_1)(1 + \cos^2\Theta) + 2(A_e + \xi_2)A_\tau \cos\Theta} \quad \text{as} \quad \beta_\tau \rightarrow 1. \quad (51)$$

From the statistics point of view it is worthwhile to deal with the degree of polarization multiplied with the angular distribution and then integrated over the polar angle

$$P_\tau = \frac{1}{\sigma_{pol}} \int P_\tau(\theta) \frac{d\sigma_{pol}}{d\cos\Theta} d\cos\Theta = -\frac{4\beta_\tau}{3 + \beta_\tau^2 + 3\eta_\tau(1 - \beta_\tau^2)} A_\tau \Rightarrow -A_\tau \text{ as } \beta_\tau \rightarrow 1, \quad (52)$$

that turns out to be independent of the initial electron and positron polarization as well as the eeZ couplings.

Let us now discuss how the π^- spectra arising from the two-stage two-body decays

$$\tau^- \rightarrow \rho^- \nu_\tau \rightarrow (\pi^- \pi^0) \nu_\tau \quad (53)$$

can be used to determine the polarization of the vector meson ρ^- , acting as a polarization analyzer of the parent particle τ^- [54]. The decay mode $\tau^- \rightarrow \rho^- \nu_\tau$ accounts for approximately 22% of all τ decays. Adopting the helicity formalism, the transition amplitude of the process $\tau^- \rightarrow \rho^- \nu_\tau$ are given by

$$A[\tau^-(p, \sigma_\tau) \rightarrow \rho^-(q, \lambda) \nu_\tau(k, -)] = \sqrt{2} G_F g_\rho [\bar{u}(k, -) \gamma^\mu P_L u(p, \sigma_\tau)] \epsilon_\mu^*(q, \lambda), \quad (54)$$

with $P_L = (1 - \gamma_5)/2$. The helicity amplitude can be cast into the normalized form in the τ^- rest frame as

$$D_{\sigma_\tau; -}(\theta_\rho, \phi_\rho) = \frac{\sqrt{2} m_\rho}{\sqrt{m_\tau^2 + 2m_\rho^2}} d_{\sigma_\tau, -1/2}^{1/2}(\theta_\rho) e^{i\sigma_\tau \phi_\rho}, \quad (55)$$

$$D_{\sigma_\tau; 0}(\theta_\rho, \phi_\rho) = \frac{m_\tau}{\sqrt{m_\tau^2 + 2m_\rho^2}} d_{\sigma_\tau, 1/2}^{1/2}(\theta_\rho) e^{i\sigma_\tau \phi_\rho}. \quad (56)$$

Note that the decay with the ρ^- helicity of $\lambda = +1$ is forbidden due to the angular momentum conservation. Folding the polarized τ^- decay distributions with a given τ^- polarization matrix and integrating them over the azimuthal angle ϕ_ρ yield the polar-angle dependent distributions in the $(0, -1)$ basis

$$W_{\sigma\lambda}(\theta_\rho) = \begin{bmatrix} \frac{m_\tau^2}{m_\tau^2 + 2m_\rho^2} (1 + P_\tau \cos \theta_\rho) & -\frac{\sqrt{2} m_\tau m_\rho}{m_\tau^2 + 2m_\rho^2} P_\tau \sin \theta_\rho \\ -\frac{\sqrt{2} m_\tau m_\rho}{m_\tau^2 + 2m_\rho^2} P_\tau \sin \theta_\rho & \frac{2m_\rho^2}{m_\tau^2 + 2m_\rho^2} (1 - P_\tau \cos \theta_\rho) \end{bmatrix}, \quad (57)$$

apart from an overall factor. The average of the diagonal elements is the normalized polar-angle distribution of ρ^- in the τ^- rest frame

$$\overline{W}(\theta_\rho) = \frac{1}{2} \left[1 + \left(\frac{m_\tau^2 - 2m_\rho^2}{m_\tau^2 + 2m_\rho^2} \right) P_\tau \cos \theta_\rho \right]. \quad (58)$$

The polarization-dependent distribution matrix in Eq. (57) cannot be directly used before being combined with the ρ decay part, but it first must be transformed by the Wick helicity rotation into the corresponding polarization-dependent distribution in the e^-e^+ CM frame, i.e. the LAB frame as

$$W'_{\sigma'\lambda'}(\omega, \theta_\rho) = \sum_{\sigma, \lambda} d_{\sigma'\sigma}^1(\omega) d_{\lambda'\lambda}^1(\omega) W_{\sigma\lambda}(\theta_\rho). \quad (59)$$

Although it is straightforward to derive the full expression of the distribution matrix in the LAB, we restrict ourselves to the diagonal elements, since we consider only the polar-angle distributions and a parity-conserving decay $\rho^- \rightarrow \pi^- \pi^0$. An explicit evaluation leads to the following transverse and longitudinal

distributions of the ρ^- meson,

$$W'_T(\omega, \theta_\rho) = \frac{m_\tau^2 + m_\rho^2}{m_\tau^2 + 2m_\rho^2} - \frac{m_\tau^2 - m_\rho^2}{m_\tau^2 + 2m_\rho^2} \cos^2 \omega + P_\tau \left[\left(\frac{m_\tau^2 - m_\rho^2}{m_\tau^2 + 2m_\rho^2} - \frac{m_\tau^2 + m_\rho^2}{m_\tau^2 + 2m_\rho^2} \cos^2 \omega \right) \cos \theta_\rho - \frac{2m_\tau m_\rho}{m_\tau^2 + 2m_\rho^2} \cos \omega \sin \omega \sin \theta_\rho \right], \quad (60)$$

$$W'_L(\omega, \theta_\rho) = \frac{m_\rho^2}{m_\tau^2 + 2m_\rho^2} + \frac{m_\tau^2 - m_\rho^2}{m_\tau^2 + 2m_\rho^2} \cos^2 \omega - P_\tau \left[\left(\frac{m_\rho^2}{m_\tau^2 + 2m_\rho^2} - \frac{m_\tau^2 + m_\rho^2}{m_\tau^2 + 2m_\rho^2} \cos^2 \omega \right) \cos \theta_\rho - \frac{2m_\tau m_\rho}{m_\tau^2 + 2m_\rho^2} \cos \omega \sin \omega \sin \theta_\rho \right], \quad (61)$$

in the LAB frame to be folded *directly* with the ρ^- decay distributions in the ρ^- rest frame.

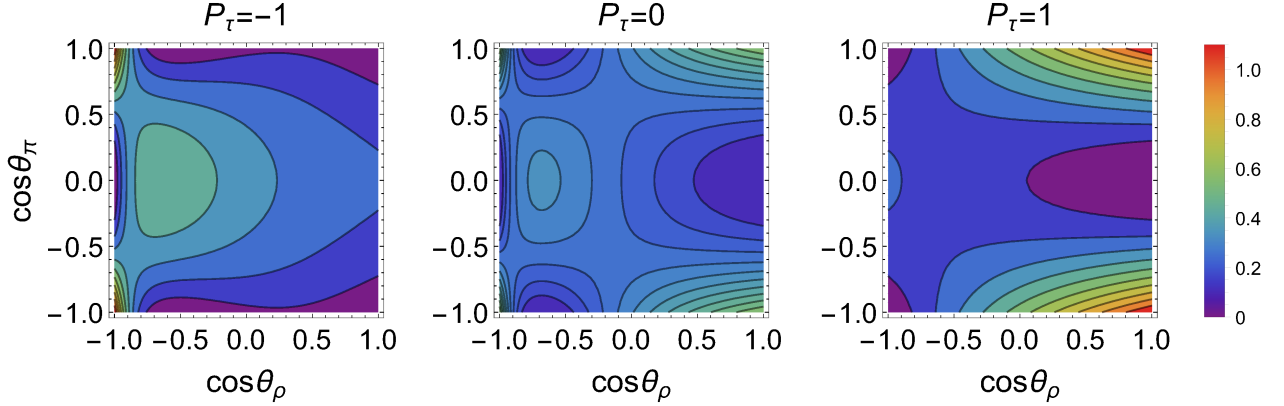


Figure 4: Contour plots of the polar-angle correlation function $d^2\mathcal{C}(\theta_\rho, \theta_\pi)/d \cos \theta_\rho d \cos \theta_\pi$ for $P_\tau = -1$ (left), $P_\tau = 0$ (middle) and $P_\tau = 1$ (right) of the decaying τ longitudinal polarization. Here, the e^+e^- CM energy is set to the Z mass $m_Z = 91$ GeV and $m_\tau = 1.78$ GeV and $m_\rho = 0.77$ GeV are chosen.

The ρ^- decays via $\rho^- \rightarrow \pi^- \pi^0$ with almost 100% probability. By the conserved vector current (CVC) hypothesis [56, 57], the ρ^- decay mode can be completely described by the four-vector current as

$$D[\rho^- \rightarrow \pi^- \pi^0] = f_\rho (p_{\pi^-} - p_{\pi^0})_\mu \epsilon^\mu, \quad (62)$$

where ϵ^μ is the ρ^- polarization vector. The helicity amplitudes can be cast into the simple form in the helicity basis

$$D_{\sigma_\rho}(\theta_\pi, \phi_\pi) \sim d_{\sigma_\rho, 0}^1(\theta_\pi) e^{i\sigma_\rho \phi_\pi}, \quad (63)$$

in the ρ^- rest frame, leading to the decay angular distributions [54] for the transversely and longitudinally polarized ρ^-

$$\frac{1}{\Gamma} \frac{d\Gamma(\rho_T \rightarrow 2\pi)}{d \cos \theta_\pi} = \frac{3}{8} \sin^2 \theta_\pi, \quad (64)$$

$$\frac{1}{\Gamma} \frac{d\Gamma(\rho_L \rightarrow 2\pi)}{d \cos \theta_\pi} = \frac{3}{4} \cos^2 \theta_\pi, \quad (65)$$

with $\cos \theta_\pi = (2E_\pi/E_\rho - 1)/\sqrt{1 - 4m_\pi^2/m_\rho^2}$ in the collinear limit.

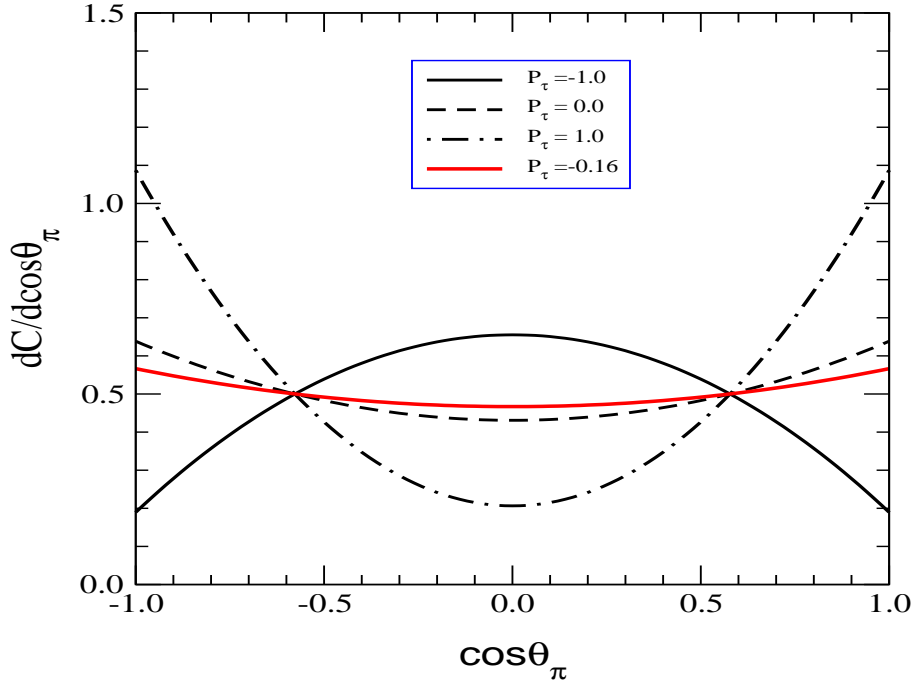


Figure 5: Polar angle distribution $d\mathcal{C}/d\cos\theta_\pi$ in the two-stage decay $\tau^- \rightarrow \rho^- \nu_\tau \rightarrow (\pi^- \pi^0) \nu_\tau$ for the degrees of τ polarization of $P_\tau = \pm 1, 0$ (taken simply for comparison) and $P_\tau = -0.16$, the value expected with the SM couplings.

Eventually, combining Eqs. (60) and (61) with Eqs. (64) and (65) we can obtain the full normalized spin and polar-angle correlations of the two-stage decays $\tau^- \rightarrow \rho^- \nu_\tau \rightarrow (\pi^- \pi^0) \nu_\tau$:

$$\frac{d^2\mathcal{C}}{d\cos\theta_\rho d\cos\theta_\pi} = \frac{1}{4} \left[f(\theta_\rho, \theta_\pi) + P_\tau g(\theta_\rho, \theta_\pi) \right], \quad (66)$$

with the functions containing the $(\theta_\rho, \theta_\pi)$ correlations given by

$$f(\theta_\rho, \theta_\pi) = 1 + \frac{1}{2} \frac{m_\tau^2 - m_\rho^2}{m_\tau^2 + 2m_\rho^2} (3 \cos^2 \omega - 1)(3 \cos^2 \theta_\pi - 1), \quad (67)$$

$$g(\theta_\rho, \theta_\pi) = \frac{m_\tau^2 - 2m_\rho^2}{m_\tau^2 + 2m_\rho^2} \cos \theta_\rho + \frac{1}{2} \frac{m_\tau^2 + m_\rho^2}{m_\tau^2 + 2m_\rho^2} (3 \cos^2 \omega - 1) \cos \theta_\rho (3 \cos^2 \theta_\pi - 1) + 3 \frac{m_\tau m_\rho}{m_\tau^2 + 2m_\rho^2} \cos \omega \sin \omega \sin \theta_\rho (3 \cos^2 \theta_\pi - 1), \quad (68)$$

which are consistent with the corresponding expressions in Refs. [54,58]. We note that the Wick helicity rotation angle ω is a function of θ_ρ , the polar angle of ρ^- in the τ^- rest frame and it depends on β_τ in the LAB and β_ρ fixed with the τ and ρ masses. Thus P_τ can be determined from an analysis of the two-dimensional distribution with greatly improved precision as demonstrated numerically in Fig. 4.

If the correlation function in Eq. (66) is integrated over the polar angle θ_ρ of the ρ^- , then we obtain the single polar angle distribution $d\mathcal{C}/d\cos\theta_\pi$ of π^- expressed in terms of PEFs described in detail in Appendix C. In this case with $\beta_\tau \simeq 1$, the asymptotic expressions of PEFs can be safely used. We note that

the polar-angle distribution, symmetric due to the parity-preserving decay $\rho^- \rightarrow \pi^- \pi^0$, is quite sensitive to the value of P_τ as clearly indicated by Fig. 5. Nevertheless, it is certain that the full polar-angle correlation enables us to determine P_τ and so the weak-mixing angle θ_W with greater precision.

5.2 The process $e^- e^+ \rightarrow t \bar{t}$ followed by $t \rightarrow W^+ b$ and $W^+ \rightarrow \ell^+ \nu_\ell$

Studying top quarks with great precision after its discovery at Tevatron [59, 60] is important in particular for several theoretical and experimental reasons. It allows us to probe physics at a much higher mass scale than the other SM fermions. To a very good approximation the top quark decays as a free quark, because of the top quark lifetime of about 4.7×10^{-25} s (corresponding to the width of 1.41 GeV) is too short for the top quark to bind with light quarks before it decays [61]. Furthermore, the maximally parity-violating two-body top-quark decay $t \rightarrow W^+ b$ enables us to analyze the top-quark polarization efficiently, which is in general non-zero if its production proceeds through some parity-violating interactions [38, 39, 62–74].

In this subsection, as another characteristic example of the spin combination $1/2 \rightarrow 1 + 1/2$, we consider the following three-stage top production and decay processes at the tree level in the SM:

$$e^- e^+ \rightarrow t \bar{t} \rightarrow (W^+ b) \bar{t} \rightarrow ([\ell^+ \nu_\ell] b) \bar{t}, \quad (69)$$

including the two-body decay $t \rightarrow W^+ b$ as the key chain, with $\ell = e, \mu$, while treating \bar{t} inclusively.

The t -pair production in $e^- e^+$ annihilation proceeds via two s -channel γ and Z exchanges. The Feynman rules of the eeV and Vtt couplings with $V = \gamma, Z$ are

$$\langle \gamma^\mu | e^- e^+ \rangle = ie \gamma^\mu, \quad (70)$$

$$\langle t \bar{t} | \gamma_\mu \rangle = -ie Q_t \gamma_\mu, \quad (71)$$

$$\langle Z^\mu | e^- e^+ \rangle = ig_Z \gamma^\mu (v_e - a_e \gamma_5), \quad (72)$$

$$\langle t \bar{t} | Z_\mu \rangle = ig_Z \gamma_\mu (v_t - a_t \gamma_5), \quad (73)$$

with the normalized t electric charge $Q_t = 2/3$ and the vector and axial-vector couplings $v_t = 1/4 - 2s_W^2/3$ and $a_t = 1/4$.

By introducing four bilinear charges [75, 76] defined by

$$Q_{\pm\pm} = Q_t - \frac{\gamma_Z(s)}{c_W^2 s_W^2} (v_e \mp a_e)(v_t \mp a_t), \quad (74)$$

$$Q_{\pm\mp} = Q_t - \frac{\gamma_Z(s)}{c_W^2 s_W^2} (v_e \mp a_e)(v_t \pm a_t), \quad (75)$$

with $\gamma_Z(s) = s/(s - m_Z^2 + im_Z \Gamma_Z)$, the helicity amplitudes in the $e^- e^+$ CM frame can be written in a compact form as

$$T(\sigma \bar{\sigma} : \lambda \bar{\lambda}) = -2\pi\alpha \delta_{\bar{\sigma}, -\sigma} \langle \sigma : \lambda \bar{\lambda} \rangle e^{i(\sigma - \bar{\sigma})\Phi}, \quad (76)$$

with the replacement $e^2 = 4\pi\alpha$ by the fine-structure constant α and with $m_e = 0$ assumed, where the helicity-dependent parts [62] are

$$\langle \pm : ++ \rangle = \mp (1 - \beta_t^2)^{1/2} (Q_{\pm\pm} + Q_{\pm-}) \sin \Theta, \quad (77)$$

$$\langle \pm : +- \rangle = [(1 + \beta_t) Q_{\pm\pm} + (1 - \beta_t) Q_{\pm-}] (1 \pm \cos \Theta), \quad (78)$$

$$\langle \pm : -+ \rangle = [(1 - \beta_t) Q_{\pm\pm} + (1 + \beta_t) Q_{\pm-}] (1 \mp \cos \Theta), \quad (79)$$

$$\langle \pm : -- \rangle = \mp (1 - \beta_t^2)^{1/2} (Q_{\pm\pm} + Q_{\pm-}) \sin \Theta. \quad (80)$$

We note that the non-zero Z width can in general be neglected for the energies considered in the present analysis so that the bilinear charges are real with very good approximation at the tree level.

For the sake of notational convenience we introduce six quartic charges [75, 76] for the t -pair production process. These charges correspond to independent helicity-dependent components describing the t -pair production for polarized electrons and positrons with negligible electron mass. Three parity-even (unprimed) quartic charges are defined in terms of bilinear charges as

$$Q_1 = \frac{1}{4} (|Q_{++}|^2 + |Q_{+-}|^2 + |Q_{-+}|^2 + |Q_{--}|^2) , \quad (81)$$

$$Q_2 = \frac{1}{2} \text{Re} (Q_{++} Q_{+-}^* + Q_{--} Q_{-+}^*) , \quad (82)$$

$$Q_3 = \frac{1}{4} (|Q_{++}|^2 - |Q_{+-}|^2 - |Q_{-+}|^2 + |Q_{--}|^2) , \quad (83)$$

and three parity-odd (primed) quartic charges as

$$Q'_1 = \frac{1}{4} (|Q_{++}|^2 + |Q_{+-}|^2 - |Q_{-+}|^2 - |Q_{--}|^2) , \quad (84)$$

$$Q'_2 = \frac{1}{2} \text{Re} (Q_{++} Q_{+-}^* - Q_{--} Q_{-+}^*) , \quad (85)$$

$$Q'_3 = \frac{1}{4} (|Q_{++}|^2 - |Q_{+-}|^2 + |Q_{-+}|^2 - |Q_{--}|^2) . \quad (86)$$

In terms of these six quartic charges, the differential cross section for longitudinally polarized electron and positron beams and the degree of longitudinal t polarization are given in a simple form by

$$\frac{d\sigma_{\text{pol}}}{d\cos\Theta} = \frac{\pi\alpha^2}{2s} \beta_t [(1 - P_{e^-} P_{e^+}) \Sigma_{\text{unp}} + (P_{e^-} - P_{e^+}) \Sigma_{LL}] , \quad (87)$$

$$P_t(\Theta) = \frac{(1 - P_{e^-} P_{e^+}) \Delta_{\text{unp}} + (P_{e^-} - P_{e^+}) \Delta_{LL}}{(1 - P_{e^-} P_{e^+}) \Sigma_{\text{unp}} + (P_{e^-} - P_{e^+}) \Sigma_{LL}} . \quad (88)$$

The polar-angle dependent coefficients, Σ_{unp} , Σ_{LL} , Δ_{unp} and Δ_{LL} , appearing in Eqs. (87) and (88) are expressed in terms of the quartic charges as

$$\Sigma_{\text{unp}} = (1 + \beta_t^2 \cos^2 \Theta) Q_1 + (1 - \beta_t^2) Q_2 + 2\beta_t Q_3 \cos \Theta , \quad (89)$$

$$\Sigma_{LL} = (1 + \beta_t^2 \cos^2 \Theta) Q'_1 + (1 - \beta_t^2) Q'_2 + 2\beta_t Q'_3 \cos \Theta , \quad (90)$$

$$\Delta_{\text{unp}} = [(1 + \beta_t^2) Q'_1 + (1 - \beta_t^2) Q'_2] \cos \Theta + \beta_t Q'_3 (1 + \cos^2 \Theta) , \quad (91)$$

$$\Delta_{LL} = [(1 + \beta_t^2) Q_1 + (1 - \beta_t^2) Q_2] \cos \Theta + \beta_t Q_3 (1 + \cos^2 \Theta) . \quad (92)$$

If the production angles could be measured unambiguously on an event-by-event basis, the quartic charges could be extracted directly from the angular dependence of the cross section equipped with polarized electron and/or positron beams at a single energy and similarly from the direct measurement of longitudinal t polarization. However, the (longitudinal) t polarization can only be determined indirectly from angular distribution of decay products if the t decay dynamics is known.

The top quark t with its mass of about 173 GeV decays via the parity-violating weak decay $t \rightarrow W^+ b$ with almost 100% probability [55], of which the dynamical structure is identical to that of $\tau^- \rightarrow \rho^- \nu_\tau$. The decay mode with W^+ of helicity +1 in the t rest frame is forbidden because of angular momentum conservation. Thus folding the polarized t decay distributions with a given t polarization matrix and integrating the

resulting distributions over the W^+ azimuthal angle yield the polar-angle dependent distributions in the $(0, -1)$ basis of W^+ , while ignoring the $+1$ mode with vanishing components, as

$$W_{\sigma\lambda}(\theta_W) = \begin{bmatrix} \frac{m_t^2}{m_t^2 + 2m_W^2}(1 + P_t \cos \theta_W) & -\frac{\sqrt{2}m_t m_W}{m_t^2 + 2m_W^2} P_t \sin \theta_W \\ -\frac{\sqrt{2}m_t m_W}{m_t^2 + 2m_W^2} P_t \sin \theta_W & \frac{2m_W^2}{m_t^2 + 2m_W^2}(1 - P_t \cos \theta_W) \end{bmatrix}, \quad (93)$$

of which the average of the diagonal elements leads to the normalized polar-angle distribution of W^+ in the t rest frame:

$$\overline{W}(\theta_W) = \frac{1}{2} \left[1 + \left(\frac{m_t^2 - 2m_W^2}{m_t^2 + 2m_W^2} \right) P_t \cos \theta_W \right]. \quad (94)$$

In order to connect the W^+ polarization density matrix in the t rest frame directly with the W^+ decay distribution in the W^+ rest frame, it is necessary to transform the density matrix in Eq. (93) by Wick helicity rotation. Although it is straightforward to derive the full expression of the matrix in the e^-e^+ CM frame, we will restrict ourselves to the derivation of the diagonal elements. An explicit calculation leads to the following distributions

$$W'_{\pm\pm}(\omega, \theta_W) = \frac{1}{2} [W'_T(\omega, \theta_W) \pm Z'_T(\omega, \theta_W)], \quad (95)$$

$$W'_{00}(\omega, \theta_W) = W'_L(\omega, \theta_W), \quad (96)$$

with the parity-even and parity-odd transverse parts, W'_T and Z'_T , given explicitly by

$$W'_T(\omega, \theta_W) = \frac{m_t^2 + m_W^2}{m_t^2 + 2m_W^2} - \frac{m_t^2 - m_W^2}{m_t^2 + 2m_W^2} \cos^2 \omega \\ + P_t \left[\left(\frac{m_t^2 + m_W^2}{m_t^2 + 2m_W^2} - \frac{m_t^2 + m_W^2}{m_t^2 + 2m_W^2} \cos^2 \omega \right) \cos \theta_W - \frac{2m_t m_W}{m_t^2 + 2m_W^2} \cos \omega \sin \omega \sin \theta_W \right], \quad (97)$$

$$Z'_T(\omega, \theta_W) = -\frac{2m_W^2}{m_t^2 + 2m_W^2} \cos \omega + 2P_t \left(\frac{m_W^2}{m_t^2 + 2m_W^2} \cos \omega \cos \theta_W + \frac{m_t m_W}{m_t^2 + 2m_W^2} \sin \omega \sin \theta_W \right), \quad (98)$$

and the parity-even longitudinal part W'_L given explicitly by

$$W'_L(\omega, \theta_W) = \frac{m_W^2}{m_t^2 + 2m_W^2} + \frac{m_t^2 - m_W^2}{m_t^2 + 2m_W^2} \cos^2 \omega \\ - P_t \left[\left(\frac{m_W^2}{m_t^2 + 2m_W^2} - \frac{m_t^2 + m_W^2}{m_t^2 + 2m_W^2} \cos^2 \omega \right) \cos \theta_W - \frac{2m_t m_W}{m_t^2 + 2m_W^2} \cos \omega \sin \omega \sin \theta_W \right], \quad (99)$$

in the LAB to be folded with the W^+ decay distributions in the W^+ rest frame boosted directly back from the LAB.

The W^+ weak decay into a positive lepton ℓ^+ and its neutrino ν_ℓ with $\ell = e$ or μ , accounting for the branching fraction of about 20%, is a very clean signal for diagnosing the W^+ polarization. Neglecting the lepton mass with good approximation, i.e. setting $m_\ell = 0$, we can obtain the decay helicity amplitudes in the W^+ rest frame as

$$D_{\sigma_W}(\theta_\ell, \phi_\ell) = \frac{g}{\sqrt{2}} \bar{u}(k, -) \gamma^\mu P_L v(q, +) \epsilon_\mu(p, \sigma) = g m_W d_{\sigma_W, 1}^1(\theta_\ell) e^{i\sigma_W \phi_\ell}, \quad (100)$$

leading to the normalized amplitudes

$$D_{\pm}(\theta_\ell, \phi_\ell) = \frac{1 \pm \cos \theta_\ell}{2} e^{\pm i\phi_\ell}, \quad (101)$$

$$D_0(\theta_\ell, \phi_\ell) = \frac{\sin \theta_\ell}{\sqrt{2}}, \quad (102)$$

satisfying $|D_+|^2 + |D_0|^2 + |D_-|^2 = 1$. Combining Eqs. (95) and (96) with Eqs. (101) and (102) yields the full spin and polar-angle correlations of the two-stage decays $t \rightarrow W^+ b \rightarrow (\ell^+ \nu_\ell) b$:

$$\frac{d^2\mathcal{C}}{d \cos \theta_W d \cos \theta_\ell} = \frac{1}{4} \left[f(\theta_W, \theta_\ell) + P_t g(\theta_W, \theta_\ell) \right], \quad (103)$$

with the two θ_W and θ_ℓ correlation functions of which the first function

$$f(\theta_W, \theta_\ell) = 1 - \frac{3m_W^2}{m_t^2 + 2m_W^2} \cos \omega \cos \theta_\ell - \frac{1}{4} \frac{m_t^2 - m_W^2}{m_t^2 + 2m_W^2} (3 \cos^2 \omega - 1)(3 \cos^2 \theta_\ell - 1), \quad (104)$$

surviving even for unpolarized t and the second function

$$\begin{aligned} g(\theta_W, \theta_\ell) &= \frac{m_t^2 - 2m_W^2}{m_t^2 + 2m_W^2} \cos \theta_W + \frac{3m_W^2}{m_t^2 + 2m_W^2} \cos \omega \cos \theta_W \cos \theta_\ell \\ &\quad - \frac{1}{4} \frac{m_t^2 + m_W^2}{m_t^2 + 2m_W^2} (3 \cos^2 \omega - 1) \cos \theta_W (3 \cos^2 \theta_\ell - 1) \\ &\quad + \frac{3m_t m_W}{m_t^2 + 2m_W^2} \sin \omega \sin \theta_W \cos \theta_\ell - \frac{1}{2} \frac{3m_t m_W}{m_t^2 + 2m_W^2} \cos \omega \sin \omega \sin \theta_W (3 \cos^2 \theta_\ell - 1), \end{aligned} \quad (105)$$

contributing only when the t quark is polarized. As mentioned before, the Wick helicity rotation angle ω is a function of θ_W , the polar angle of W^+ in the t rest frame, and two boost factors, β_t and $\beta_W = (m_t^2 - m_W^2)/(m_t^2 + m_W^2)$. Thus P_t can be determined efficiently from an analysis of the two-dimensional angular distribution as demonstrated clearly with three values of $P_t = \pm 1, 0$ (for the sake of simple comparison) at the $e^- e^+$ CM energy of 500 GeV in Fig. 6.

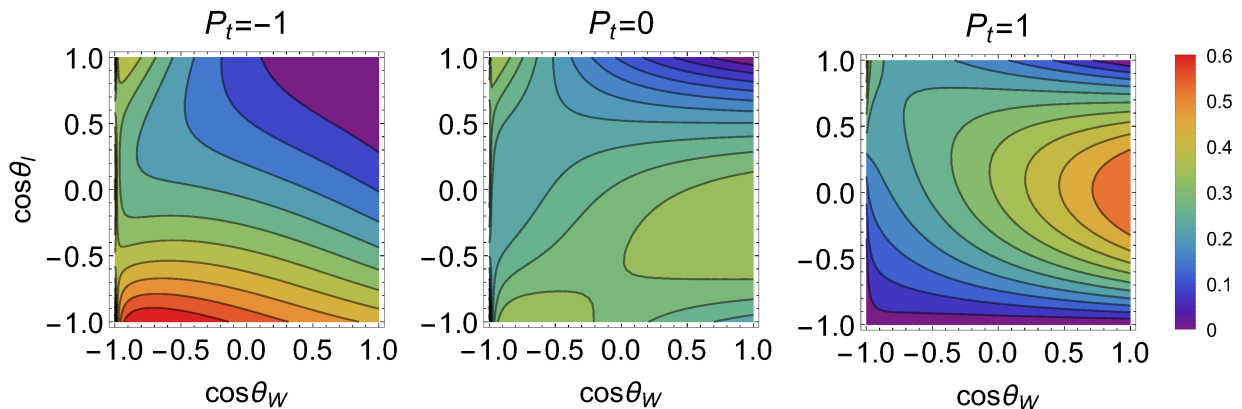


Figure 6: Contour plots of the polar-angle correlation function $d^2\mathcal{C}/d \cos \theta_W d \cos \theta_\ell$ for $P_t = 1$ (left), $P_t = 0$ (middle), and $P_t = -1$ (right) values of the decaying t longitudinal polarization. Here, the $e^+ e^-$ CM energy of 500 GeV is taken and $m_t = 173$ GeV and $m_W = 80.4$ GeV are assumed.

If the correlation function in Eq. (103) is integrated over the polar angle θ_W of the W^+ , then we can obtain the single polar angle distribution $d\mathcal{C}/d \cos \theta_\ell$ of ℓ^- expressed in terms of polarization estimators described in detail in appendix C. We note that the polar-angle distribution, asymmetric due to the parity-violating decay $W^+ \rightarrow \ell^+ \nu_\ell$, is quite sensitive to the value of P_t as shown in Fig. 7. Nevertheless, as mentioned before, it is certain that the full polar-angle correlation enables us to determine P_t and so the weak-mixing angle θ_W with better precision.

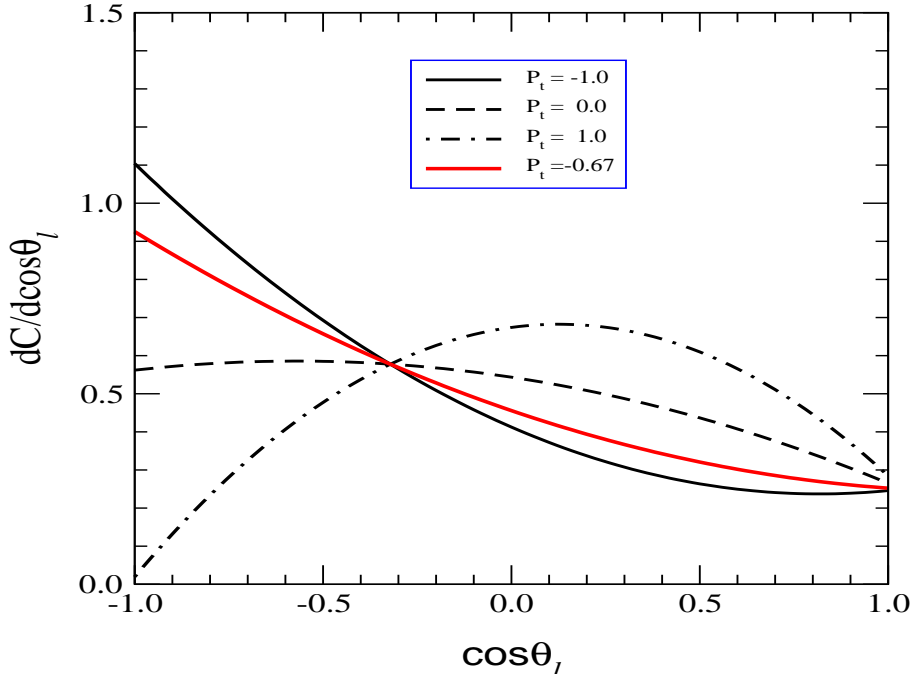


Figure 7: Polar angle distribution $dC/d\cos\theta_\ell$ in the two-stage decay $t \rightarrow W^+b \rightarrow (\ell^+\nu_\ell)t$ for the degrees of τ polarization of $P_t = \pm 1, 0$ for the sake of simple comparison and $P_t = -0.67$, the value expected with the SM γ and Z couplings to a pair of top quarks.

5.3 The decay $T \rightarrow Zt$ of a heavy vectorlike top quark T , followed by $Z \rightarrow \ell^-\ell^+$

In many models of new physics beyond the SM such as extra-dimensional models and little Higgs models [77–86], there are heavy vectorlike fermions which decay to the SM fermions plus a gauge boson (W^\pm and Z) or a Higgs boson (H). The mixing of vector-like quarks with the third generation and in particular with the top quark is a common feature in little Higgs models and it may be sizable.

Due to its heavy mass, the new colored vectorlike heavy fermion T may only be produced at high energy hadron colliders. The apparent production processes are the QCD pair production, $q\bar{q}, gg \rightarrow T\bar{T}$, producing unpolarized T particles. However, the phase space suppression for the heavy TeV-scale mass is rather severe in the pair production. In contrast, the single T production via W exchange in t -channel (or Wb fusion) $qb \rightarrow Tq'$, in which the particle T is produced in a polarized state, falls off much more slowly with the T mass and takes over for m_T larger than a few hundred GeV. According to the so-called Goldstone boson equivalence theorem [87, 88], the T couplings to the longitudinally polarized gauge bosons are not suppressed, rendering the decay $T \rightarrow Zt$ being one of the main decay channels. The Z boson in the final state gives an unambiguous event identification via its clean leptonic decay, and the system $t(\rightarrow Wb)Z$ enables us to reconstruct m_T [85].

Without taking any specific model into account, we assume a generic chiral structure for the TtZ interaction vertex of a heavy and SM top quarks, T and t , and the neutral gauge boson Z , denoting the vector and axial-vector couplings by v_T and a_T normalized with the SM gauge coupling $g_Z = e/c_W s_W$ as

$$\langle t|Z|T\rangle_\mu = -ig_Z \gamma_\mu (v_T - a_T \gamma_5). \quad (106)$$

The helicity amplitude of the two-body decay $T \rightarrow Zt$ with its expected branching fraction larger than 20%

is written in the T rest frame as

$$D_{\sigma_T; \lambda, \sigma_t}(\theta_Z, \phi_Z) = F_{\lambda \sigma_t}^{1/2} d_{\sigma_T, \lambda - \sigma_t}^{1/2}(\theta_Z) e^{i \sigma_T \phi_Z}, \quad (107)$$

where θ_Z and ϕ_Z are the polar and azimuthal angles of the Z boson. Apart from an overall factor, the angle-independent reduced helicity amplitudes read

$$F_{\pm\pm}^{1/2} = \sqrt{2}(v_1 \mp a_1) \quad \text{and} \quad F_{0\pm}^{1/2} = \sqrt{2}(v_0 \mp a_0), \quad (108)$$

in terms of the redefined vector and axial-vector couplings as

$$v_1 = \sqrt{(1 - \mu_t)^2 - \mu_Z^2} v_T, \quad a_1 = \sqrt{(1 + \mu_t)^2 - \mu_Z^2} a_T, \quad (109)$$

$$v_0 = \frac{(1 + \mu_t)}{\sqrt{2}\mu_Z} \sqrt{(1 - \mu_t)^2 - \mu_Z^2} v_T, \quad a_0 = \frac{(1 - \mu_t)}{\sqrt{2}\mu_Z} \sqrt{(1 + \mu_t)^2 - \mu_Z^2} a_T, \quad (110)$$

with the normalized dimensionless mass ratios, $\mu_t = m_t/m_T$ and $\mu_Z = m_Z/m_T$.

Integrating the decay distribution derived from the helicity amplitudes over the azimuthal angle ϕ_Z and folding with the T polarization P^T yield the helicity-dependent distributions⁶

$$\mathcal{D}_{\pm\pm}(\theta_Z) = |v_1 \mp a_1|^2 (1 \pm P^T \cos \theta_Z), \quad (111)$$

$$\mathcal{D}_{\pm\mp}(\theta_Z) = 0, \quad (112)$$

$$\mathcal{D}_{+0}(\theta_Z) = \mathcal{D}_{0+}^* = -(v_1 - a_1)(v_0 - a_0)^* P^T \sin \theta_Z, \quad (113)$$

$$\mathcal{D}_{-0}(\theta_Z) = \mathcal{D}_{0-}^* = -(v_1 + a_1)(v_0 + a_0)^* P^T \sin \theta_Z, \quad (114)$$

$$\mathcal{D}_{00}(\theta_Z) = 2(|v_0|^2 + |a_0|^2) + 4\text{Re}(v_0 a_0^*) P^T \cos \theta_Z, \quad (115)$$

apart from an overall factor. The average of the diagonal elements leads to the normalized polar-angle distribution in the T rest frame:

$$\overline{W}(\theta_Z) = \frac{1}{2} (1 + A P^T \cos \theta_Z) \quad \text{with} \quad A = \frac{2 \text{Re}(v_0 a_0^* - v_1 a_1^*)}{|v_1|^2 + |a_1|^2 + |v_0|^2 + |a_0|^2}. \quad (116)$$

In order to connect the Z polarization density matrix in the T rest frame *directly* with the Z decay distribution in the LAB we transform it into the Z density matrix in the LAB by Wick helicity rotation. Although it is straightforward to derive the full expression in any given LAB, in the present work we restrict ourselves to the derivation of the diagonal elements for a fixed T speed, β_T . As the transformed distributions involve various combinations of the redefined couplings, $\{v_1, a_1, v_0, a_0\}$, let us first introduce five ratios consisting of three parity-odd ratios

$$A_1 = -\frac{2 \text{Re}(v_1 a_1^*)}{|v_1|^2 + |a_1|^2 + |v_0| + |a_0|^2}, \quad (117)$$

$$A_2 = -\frac{2 \text{Re}(v_1 a_0^* + a_1 v_0^*)}{|v_1|^2 + |a_1|^2 + |v_0| + |a_0|^2}, \quad (118)$$

$$A_3 = -\frac{2 \text{Re}(v_1 a_1^* + 2v_0 a_0^*)}{|v_1|^2 + |a_1|^2 + |v_0| + |a_0|^2}, \quad (119)$$

and two parity-even ratios

$$\eta_1 = \frac{|v_1|^2 + |a_1|^2 - 2|v_0|^2 - 2|a_0|^2}{|v_1|^2 + |a_1|^2 + |v_0|^2 + |a_0|^2}, \quad (120)$$

$$\eta_2 = \frac{2 \text{Re}(v_1 v_0^* + a_1 a_0^*)}{|v_1|^2 + |a_1|^2 + |v_0|^2 + |a_0|^2}. \quad (121)$$

⁶The reason why $\mathcal{D}_{\pm\mp} = 0$ is due to angular momentum conservation.

An explicit calculation leads to the following diagonal components of the polar-angle distributions

$$W'_{\pm\pm}(\omega, \theta_Z) = \frac{1}{2} [W'_T(\omega, \theta_Z) \pm Z'(\omega, \theta_Z)] , \quad (122)$$

$$W'_{00}(\omega, \theta_Z) = W'_L(\omega, \theta_Z) , \quad (123)$$

with the parity-even and parity-odd transverse parts, W'_T and Z'_T , and the parity-even longitudinal part W'_L given explicitly by

$$\begin{aligned} W'_T(\omega, \theta_Z) &= \frac{2}{3} + \frac{1}{3} \cos \theta_Z P^T(3A_1 - A_3) + \frac{1}{6}(3 \cos^2 \omega - 1)\eta_1 \\ &\quad + \frac{1}{6}(3 \cos^2 \omega - 1) \cos \theta_Z P^T A_3 + \frac{1}{\sqrt{2}} \cos \omega \sin \omega \sin \theta_Z P^T A_2 , \end{aligned} \quad (124)$$

$$Z'_T(\omega, \theta_Z) = \cos \omega A_1 + \frac{1}{3} \cos \omega \cos \theta_Z P^T(2 + \eta_1) + \frac{1}{\sqrt{2}} \sin \omega \sin \theta_Z P^T \eta_2 , \quad (125)$$

$$\begin{aligned} W'_L(\omega, \theta_Z) &= \frac{1}{3} + \frac{1}{6} \cos \theta_Z P^T(3A_1 - A_3) - \frac{1}{6}(3 \cos^2 \omega - 1)\eta_1 \\ &\quad - \frac{1}{6}(3 \cos^2 \omega - 1) \cos \theta_Z P^T A_3 - \frac{1}{\sqrt{2}} \cos \omega \sin \omega \sin \theta_Z P^T A_2 , \end{aligned} \quad (126)$$

in the LAB. The diagonal elements are to be folded with the Z decay distributions in the Z rest frame reconstructed directly from the LAB.

Among various decay modes of Z , the leptonic Z -boson decays $Z \rightarrow \ell^- \ell^+$, in particular, with $\ell = e$ and μ , provide us with a very clean and powerful means for reconstructing the Z -boson rest frame, independently of its production mechanism, and extracting the information on Z polarization. The normalized ℓ^- polar-angle distributions with respect to the Z polarization defined to be the Z -boson momentum direction in the LAB are given by

$$D_{\pm\pm}(\theta_\ell) = \frac{1}{4} [1 + \cos^2 \theta_\ell \mp 2A_e \cos \theta_\ell] , \quad (127)$$

$$D_{00}(\theta_\ell) = \frac{1}{2}(1 - \cos^2 \theta_\ell) . \quad (128)$$

Combining Eqs. (122) and (123) with Eqs. (127) and (128) we can obtain the full spin and polar-angle correlation of the two-stage decays $T \rightarrow Zt \rightarrow (\ell^- \ell^+)t$ as

$$\begin{aligned} \frac{d^2\mathcal{C}}{d \cos \theta_Z d \cos \theta_\ell} &= \frac{1}{4} \left[1 + \frac{1}{2} P^T(3A_1 - A_3) \cos \theta_Z - \frac{3}{2} A_e A_1 \cos \omega \cos \theta_\ell + \frac{1}{2} \eta_1 P_2(\cos \omega) P_2(\cos \theta_\ell) \right. \\ &\quad - \frac{1}{2} P^T A_e (2 + \eta_1) \cos \omega \cos \theta_Z \cos \theta_\ell - \frac{3}{2\sqrt{2}} P^T A_e \eta_2 \sin \omega \sin \theta_Z \cos \theta_\ell \\ &\quad \left. + \frac{1}{2} P^T A_3 P_2(\cos \omega) \cos \theta_Z P_2(\cos \theta_\ell) + \frac{3}{2\sqrt{2}} P^T A_2 \cos \omega \sin \omega \sin \theta_Z P_2(\cos \theta_\ell) \right] , \end{aligned} \quad (129)$$

with the second Legendre polynomial $P_2(x) = (3x^2 - 1)/2$ introduced for shortening the expression of the correlation function. As noted before, the Wick helicity rotation angle ω is a function of θ_Z , the polar angle of Z in the T rest frame, and two boost factors, β_T and β_Z .

Folding the polar-angle correlation in Eq. (129) with any given T speed distribution depending on a specific production mechanism yields the full (θ_Z, θ_ℓ) correlation in the LAB. And integrating it over the polar angle of the Z boson we obtain the single polar-angle distribution of the ℓ^- polar angle θ_ℓ .

6 Conclusions

In this work, we have provided a general and comprehensive spin analysis through polar-angle correlations in any combinations of two-stage two-body decays. *To summarize*, we have obtained the following key results from the analysis:

- * A systematic review of the Wick helicity rotation on helicity states and decay helicity amplitudes was presented.
- * Considering a two-body decay $X_2 \rightarrow YX_1$, we have described in detail how to transform through Wick helicity rotation the decay helicity amplitudes in the rest frame of the decaying particle X_2 to those in the LAB with the particle moving with non-zero speed.
- * Combining the decay $X_2 \rightarrow YX_1$ and the sequential decay $Y \rightarrow ab$, we have derived the correlated distributions expressed in terms of the Wick helicity rotation angle, the Y polar angle in the X_2 RF and the a polar angle in the YRF. They can be applicable directly in the LAB.
- * We have introduced polarization estimator functions with which all the observables depending on the X_2 polarization and the decay dynamical properties are conveniently expressed and so transparently described, even in the case when the Y direction cannot be reconstructed event by event.
- * For the sake of concrete demonstration, we have studied the characteristic tau-lepton pair polarization on the Z -boson pole and the top-quark pair production processes in e^-e^+ collisions in the framework of SM, and the decay of a heavy vectorlike top quark into a top and a Z -boson expected to occur in some models beyond the SM such as little Higgs models.
- * For completeness, all the useful formulas directly applicable for any spin and polar-angle correlations in any two-stage two-body decays are collected and explained in some detail.

Generally, a (new) heavy particle decays in a series of stages, often, including two-stage two-body decays. In this situation, the formalism presented in the present work will be very useful and powerful in determining all the particle spins in the processes and probing their dynamical properties. Based on the formalism, more interesting and concrete examples will be studied and presented in a forthcoming work.

Acknowledgments

The work was supported in part by Basic Science Research Program through the National Research Foundation (NRF) funded by the Ministry of Education, Science and Technology (NRF-2016R1D1A3B01010529) program and in part by the CERN-Korea theory collaboration.

A Wigner D - and d -functions

Let J_x, J_y, J_z be three angular momentum generators in a fixed rectangular coordinate system. The Casimir operator $J^2 = J_x^2 + J_y^2 + J_z^2$ commutes with all angular momentum generators and it can be diagonalized together with J_z , forming a complete set of orthogonal eigenstates with

$$J^2 |j\lambda\rangle = j(j+1) |j\lambda\rangle \quad \text{and} \quad J_z |j\lambda\rangle = \lambda |j\lambda\rangle, \quad (\text{A.1})$$

where $j = 0.1/2, 1, 3/2, \dots$ and $\lambda = -j, -j+1, \dots, j$ for a given j . The angular momentum operators can be used to define a three-dimensional rotation operator $\mathcal{R}(\alpha, \beta, \gamma)$ as

$$\mathcal{R}(\alpha, \beta, \gamma) = e^{-i\alpha J_z} e^{-i\beta J_y} e^{-i\gamma J_z}, \quad (\text{A.2})$$

where α, β, γ are Euler angles (characterized by the right-handed and active interpretation).

The Wigner D -functions are the matrix elements of the rotation operator \mathcal{R} in Eq. (A.2) of which the explicit form is

$$D_{\sigma,\lambda}^j(\alpha, \beta, \gamma) = \langle j\sigma | \mathcal{R}(\alpha, \beta, \gamma) | j\lambda \rangle = e^{-i\sigma\alpha} d_{\sigma,\lambda}^j(\beta) e^{-i\lambda\gamma}, \quad (\text{A.3})$$

where the mutually orthogonal Wigner d -functions are the matrix elements defined as

$$d_{\sigma,\lambda}^j(\beta) = \langle j\sigma | e^{-i\beta J_y} | j\lambda \rangle, \quad (\text{A.4})$$

which are real. By definition the orthogonal d -functions satisfy the group properties:

$$\sum_{\lambda} d_{\mu,\lambda}^j(\beta) d_{\nu,\lambda}^j(\beta) = \sum_{\sigma} d_{\sigma,\mu}^j(\beta) d_{\sigma,\nu}^j(\beta) = \delta_{\mu\nu}, \quad (\text{A.5})$$

$$d_{\sigma,\lambda}^j(\beta_1 + \beta_2) = \sum_{\mu} d_{\sigma,\mu}^j(\beta_1) d_{\mu,\lambda}^j(\beta_2), \quad (\text{A.6})$$

reflecting the characteristic additive property of two successive rotations.

For the sake of convenient discussion, the expressions of Wigner d -functions for the spin-1/2 and spin-1 cases are listed explicitly in Tab. 2.

$d_{\sigma,\lambda}^{1/2}(\theta)$		
$\sigma \backslash \lambda$	$\frac{1}{2}$	$-\frac{1}{2}$
$\frac{1}{2}$	$\cos \frac{\theta}{2}$	$-\sin \frac{\theta}{2}$
$-\frac{1}{2}$	$\sin \frac{\theta}{2}$	$\cos \frac{\theta}{2}$

$d_{\sigma,\lambda}^1(\theta)$			
$\sigma \backslash \lambda$	1	0	-1
1	$\frac{1+\cos\theta}{2}$	$-\frac{\sin\theta}{\sqrt{2}}$	$\frac{1-\cos\theta}{2}$
0	$\frac{\sin\theta}{\sqrt{2}}$	$\cos\theta$	$-\frac{\sin\theta}{\sqrt{2}}$
-1	$\frac{1-\cos\theta}{2}$	$\frac{\sin\theta}{\sqrt{2}}$	$\frac{1+\cos\theta}{2}$

Table 2: Expressions of d functions in terms of a polar angle θ for two spin values, $j = 1/2$ (left table) and $j = 1$ (right table), which are used in the present work.

The Wigner D -functions form a set of orthogonal functions of the Euler angles:

$$\int_0^{2\pi} d\alpha \int_{-1}^1 d\cos\beta \int_0^{2\pi} d\gamma D_{\sigma',\lambda'}^{j'*}(\alpha, \beta, \gamma) D_{\sigma,\lambda}^j(\alpha, \beta, \gamma) = \frac{8\pi^2}{2j+1} \delta_{j'j} \delta_{\sigma'\sigma} \delta_{\lambda'\lambda}, \quad (\text{A.7})$$

leading to the orthogonal condition for the d -functions

$$\int_{-1}^1 d\cos\beta d_{\sigma,\lambda}^{j'}(\beta) d_{\sigma,\lambda}^j(\beta) = \frac{2}{2j+1} \delta_{j'j}. \quad (\text{A.8})$$

In addition, the d -functions enjoy several symmetry properties:

$$d_{\sigma,\lambda}^j(\beta) = (-1)^{\sigma-\lambda} d_{\lambda,\sigma}^j(\beta), \quad (\text{A.9})$$

$$d_{\sigma,\lambda}^j(\beta) = d_{\lambda,\sigma}^j(-\beta), \quad (\text{A.10})$$

$$d_{\sigma,\lambda}^j(\beta) = d_{-\lambda,-\sigma}^j(\beta), \quad (\text{A.11})$$

$$d_{\sigma,\lambda}^j(\pi - \beta) = (-1)^{j+\sigma} d_{\sigma,-\lambda}^j(\beta), \quad (\text{A.12})$$

and they satisfy two useful coupling rules involving Clebsch-Gordan coefficients:

$$d_{\sigma_1, \lambda_1}^{j_1}(\beta) d_{\sigma_2, \lambda_2}^{j_2}(\beta) = \sum_{j=|j_1-j_2|}^{j_1+j_2} \langle j_1 \sigma_1 j_2 \sigma_2 | j \sigma_+ \rangle \langle j_1 \lambda_1 j_2 \lambda_2 | j \lambda_+ \rangle d_{\sigma_+, \lambda_+}^j(\beta), \quad (\text{A.13})$$

$$d_{\sigma_1, \lambda_1}^{j_1}(\beta) d_{\sigma_2, \lambda_2}^{j_2}(\beta) = \sum_{j=|j_1-j_2|}^{j_1+j_2} \langle j_1 \sigma_1 j_2, -\sigma_2 | j \sigma_- \rangle \langle j_1 \lambda_1 j_2, -\lambda_2 | j \lambda_- \rangle \\ \times (-1)^{\sigma_2 - \lambda_2} d_{\sigma_-, \lambda_-}^j(\beta), \quad (\text{A.14})$$

with the constraints $\sigma_{\pm} = \sigma_1 \pm \sigma_2$ and $\lambda_{\pm} = \lambda_1 \pm \lambda_2$. The bracket expression $\langle j_1 \mu_1 j_2 \mu_2 | j \mu \rangle$ is a Clebsch-Gordan coefficient. Two useful properties of the Clebsch-Gordan coefficients are

$$\sum_{\sigma} (-1)^{\sigma} \langle j \sigma j(-\sigma) | J 0 \rangle = (-1)^j \sqrt{2j+1} \delta_{J0} \quad \text{with} \quad \langle j \sigma j(-\sigma) | 0 0 \rangle = \frac{(-1)^{j-\sigma}}{\sqrt{2j+1}}, \quad (\text{A.15})$$

with which the orthogonality relations of d -functions can be easily derived.

B Wick helicity rotation distribution functions (WDFs)

Before exhibiting a set of WDFs defined in Eq. (20) in their explicit form for the spin values up to 1 in this appendix, we emphasize that the formalism given in the main text is so general that it can be applied to any combination of the spins, $\{j_2, j, j_1\}$, of the particles, $\{X_2, Y, X_1\}$, in the decay $X_2 \rightarrow Y X_1$ in a model-independent manner. Instead of any detailed derivations, which are demonstrated with a few examples in the main text, the essential parts for deriving WDFs and the resulting Y polarization density matrices are collected in this Appendix.

B.1 $j_2 \rightarrow 0 + j_1$

The simplest case is for the Y particle of zero spin ($j = 0$), because of no Wick helicity rotation effects at all. The (unnormalized) WDF simply reads

$$\mathcal{D}'(\omega, \theta) = \sum_{\sigma_2} \sum_{\sigma_1} \rho_{\sigma_2, \sigma_2}^{X_2} [d_{\sigma_2, -\sigma_1}^{j_2}(\theta)]^2 |F_{\sigma_1}^{j_2}|^2 \Rightarrow \langle \mathcal{D}'(\omega, \theta) \rangle = \frac{1}{(2j_2+1)} \sum_{\sigma_1}' |F_{\sigma_1}^{j_2}|^2, \quad (\text{B.1})$$

with the sum over σ_1 satisfying the constraint $|\sigma_1| \leq j_2$.

The hadronic decay processes $\Sigma \rightarrow \pi^- p$ and $\rho^- \rightarrow \pi^- \pi^0$ and any two-body decay involving a Higgs boson H belong to this category of two-body decays.

B.2 $0 \rightarrow 1/2 + 1/2$

The first non-trivial Wick helicity rotation effects show up in the case with $j_2 = 0$ and $j = j_1 = 1/2$. Two typical examples of this category are $H \rightarrow \tau^- \tau^+$ in the SM and $H^- \rightarrow \tau^- \bar{\nu}_\tau$ in a two-Higgs doublet model [89, 90].

An explicit calculation of the WDFs in this case leads to the expression:

$$\mathcal{D}'_{\sigma' \lambda'}(\omega, \theta) = \sum_{\sigma=-1/2}^{1/2} [d_{\sigma', \sigma}^{1/2}(\omega) d_{\lambda', \sigma}^{1/2}(\omega)] |F_{\sigma \sigma}^0|^2 \Rightarrow \text{Tr}(\mathcal{D}') = \sum_{\sigma} |F_{\sigma \sigma}^0|^2, \quad (\text{B.2})$$

leading to the angle-dependent 2×2 distributions, density matrix $W'(\omega, \theta)$ of the particle Y in the LAB, as

$$W'(\omega, \theta) = \frac{1}{2} \begin{pmatrix} 1 + \cos \omega A & \sin \omega A \\ \sin \omega A & 1 - \cos \omega A \end{pmatrix} \quad \text{with} \quad A = \frac{|F_{++}^0|^2 - |F_{--}^0|^2}{|F_{++}^0|^2 + |F_{--}^0|^2}, \quad (\text{B.3})$$

in the $(1/2, -1/2)$ helicity basis, where A is the Y polarization in the $X_2\text{RF}$ given in terms of the reduced helicity elements $F_{\pm\frac{1}{2}\pm\frac{1}{2}}^0$ denoted by the simplified notations $F_{\pm\pm}^0$. The diagonal elements of the Y angular distribution averaged over the polar angle θ are given by the polarization estimator $\langle \cos \omega \rangle$, of which the expressions are given in terms of β_2 and β in Appendix C and the parity-odd ratio A as

$$\rho_{\pm\pm}^Y = \frac{1}{2} \left[1 \pm \langle \cos \omega \rangle A \right]. \quad (\text{B.4})$$

For example, the decay process $H \rightarrow \tau^- \tau^+$ with a possible parity-violating $H\tau\tau$ coupling and a fixed H energy as in the Higgsstrahlung process $e^+e^- \rightarrow HZ$ is an interesting example of this decay category.

B.3 $\mathbf{0 \rightarrow 1 + 0}$

One interesting example of this type of decays is $\tilde{t}_2 \rightarrow Z\tilde{t}_1$ in the minimal supersymmetric Standard Model (MSSM), which can be realized if the mass difference between two top squarks is larger than the Z -boson mass m_Z . We note that rotational invariance forces the Z boson to be longitudinally polarized.

An explicit calculation of the WDFs in this spin-1 Y case leads to the expression:

$$\mathcal{D}'_{\sigma'\lambda'}(\omega, \theta) = [d_{\sigma',0}^1(\omega) d_{\lambda',0}^1(\omega)] |F_0^0|^2 \Rightarrow \text{Tr}(\mathcal{D}') = \sum_{\sigma} |F_{\sigma}^0|^2, \quad (\text{B.5})$$

leading to the angle-dependent 3×3 distributions, W' of the particle Y in the LAB as

$$W'(\omega, \theta) = \frac{1}{2} \begin{pmatrix} \sin^2 \omega & -\sqrt{2} \sin \omega \cos \omega & -\sin^2 \omega \\ -\sqrt{2} \sin \omega \cos \omega & 2 \cos^2 \omega & \sqrt{2} \sin \omega \cos \omega \\ -\sin^2 \omega & \sqrt{2} \sin \omega \cos \omega & \sin^2 \omega \end{pmatrix}, \quad (\text{B.6})$$

in the $(1, 0, -1)$ basis, independent of any dynamical parameters involved in the decay and also with no explicit θ -dependence. The diagonal elements of the Y angular distribution averaged over the polar angle θ are given by the PEF $\langle \cos^2 \omega \rangle$, of which the explicit form is given in Appendix C, as

$$\rho_{\pm\pm}^Y = \frac{1}{3} - \frac{1}{6} \langle 3 \cos^2 \omega - 1 \rangle \quad \text{and} \quad \rho_{00}^Y = \frac{1}{3} + \frac{1}{3} \langle 3 \cos^2 \omega - 1 \rangle. \quad (\text{B.7})$$

An example of this category is the decay process $\tilde{f}_2 \rightarrow Z\tilde{f}_1$ assuming that \tilde{f}_2 is produced in association with \tilde{f}_1^* through the process $e^+e^- \rightarrow \tilde{f}_2 \tilde{f}_1^*$ of any flavor of sfermions, which may be realized in the MSSM.

B.4 $\mathbf{0 \rightarrow 1 + 1}$

Although it is a loop-induced process and so its branching ratio is small, one important process of this decay type is the radiative decay $H \rightarrow Z\gamma$ in the SM and its extensions.

An explicit calculation of the WDFs in this case gives us the expression for the WDFs

$$\mathcal{D}'_{\sigma'\lambda'}(\omega, \theta) = \sum_{\sigma=-1}^1 [d_{\sigma',\sigma}^1(\omega) d_{\lambda',\sigma}^1(\omega)] |F_{\sigma\sigma}^0|^2 \Rightarrow \text{Tr}(\mathcal{D}') = \sum_{\sigma} |F_{\sigma\sigma}^0|^2. \quad (\text{B.8})$$

For the sake of notation, we introduce a parity-odd polarization parameter P_R and a parity-even polarization parameter as

$$A = \frac{|F_{++}^0|^2 - |F_{--}^0|^2}{|F_{++}^0|^2 + |F_{00}^0|^2 + |F_{--}^0|^2}, \quad (\text{B.9})$$

$$\eta = \frac{|F_{++}^0|^2 - 2|F_{00}^0|^2 + |F_{--}^0|^2}{|F_{++}^0|^2 + |F_{00}^0|^2 + |F_{--}^0|^2}. \quad (\text{B.10})$$

Note that $\eta = 1$ if the X_1 particle is a photon γ with no longitudinal mode. Three diagonal elements of the 3×3 density matrix ρ^Y averaged over the polar angle θ are given in terms of the parameters by

$$\rho_{\pm\pm}^Y = \frac{1}{3} \pm \frac{2}{3} \langle \cos \omega \rangle A + \frac{1}{12} \langle 3 \cos^2 \omega - 1 \rangle \eta \quad (\text{B.11})$$

$$\Rightarrow \frac{1}{3} + \frac{1}{12} \langle 3 \cos^2 \omega - 1 \rangle \pm \frac{2}{3} \langle \cos \omega \rangle A \quad \text{for } \eta = 1, \quad (\text{B.12})$$

$$\rho_{00}^Y = \frac{1}{3} - \frac{1}{6} \langle 3 \cos^2 \omega - 1 \rangle \eta \quad (\text{B.13})$$

$$\Rightarrow \frac{1}{3} - \frac{1}{6} \langle 3 \cos^2 \omega - 1 \rangle \quad \text{for } \eta = 1. \quad (\text{B.14})$$

Furthermore for the two-photon modes such as $H \rightarrow \gamma\gamma$ and $\pi^0 \rightarrow \gamma\gamma$, the longitudinal diagonal element ρ_{00}^Y cannot exist as indicated by $\eta = 1$ as well as $\omega = 0$ for massless particles.

B.5 1/2 \rightarrow 1/2 + 0

This category contains the hyperon decays, $\Lambda \rightarrow p\pi^-$ and $\Lambda \rightarrow n\pi^0$, in the SM and the decay of the second lightest neutralino, $\tilde{\chi}_2^0 \rightarrow t\tilde{t}_1^*$ in the MSSM, if kinematically allowed.

The helicity amplitude of this decay mode in the rest frame of X_2 is of the form

$$\mathcal{D}_{\sigma_2\sigma} = F_\sigma^{1/2} d_{\sigma_2\sigma}^{1/2}(\theta), \quad (\text{B.15})$$

with the X_2 and Y helicities, $\sigma_2 = \pm 1/2 = \pm$ and $\sigma = \pm 1/2 = \pm$, and the WDFs in the LAB, where the parent particle X_2 move with speed β_2 , read

$$\mathcal{D}'_{\sigma'\lambda'}(\omega, \theta) = \sum_{\sigma'_2} \sum_{\sigma, \lambda} [d_{\sigma'\sigma}^{1/2}(\omega) d_{\lambda'\lambda}^{1/2}(\omega)] [d_{\sigma'_2\sigma}^{1/2}(\theta) d_{\sigma_2\lambda}^{1/2}(\theta)] F_\sigma^{1/2} F_\lambda^{1/2*}. \quad (\text{B.16})$$

For notational convenience, we introduce a parity-odd polarization parameter A and a parity-even polarization parameter η as

$$A = \frac{|F_+^{1/2}|^2 - |F_-^{1/2}|^2}{|F_+^{1/2}|^2 + |F_-^{1/2}|^2}, \quad (\text{B.17})$$

$$\eta = \frac{2\text{Re}(F_+^{1/2} F_-^{1/2*})}{|F_+^{1/2}|^2 + |F_-^{1/2}|^2}. \quad (\text{B.18})$$

In terms of the parameters A and η can we derive two diagonal elements and thus the degree of longitudinal polarization P_L in the LAB as

$$\rho_{\pm\pm}^Y = \frac{1}{2} \left[1 \pm (\langle \cos \omega \rangle A + \langle \cos \omega \cos \theta \rangle P^{X_2} + \langle \sin \omega \sin \theta \rangle P^{X_2} \eta) \right], \quad (\text{B.19})$$

$$P_L = \langle \cos \omega \rangle A + \langle \cos \omega \cos \theta \rangle P^{X_2} + \langle \sin \omega \sin \theta \rangle P^{X_2} \eta. \quad (\text{B.20})$$

Another interesting example of this category is the decay $T \rightarrow tH$ of a new heavy top quark T into a top quark t and a Higgs boson H in the little Higgs models.

B.6 $1/2 \rightarrow 1/2 + 1$

An interesting example of this category is the decay $T \rightarrow tZ$ of a new heavy top quark T into a Z boson and a top quark t in the littlest Higgs model, one of the popular models beyond the SM.

The helicity amplitude of this decay mode in the X_2 RF is of the form

$$D_{\sigma_2; \sigma, \sigma_1} = F_{\sigma\sigma_1}^{1/2} d_{\sigma_2, \sigma - \sigma_1}^{1/2}(\theta), \quad (\text{B.21})$$

with the X_2 , X_1 and Y helicities, $\sigma_2 = \pm 1/2 = \pm$, $\sigma_1 = \pm 1, 0$, and $\sigma = \pm 1/2 = \pm$, and the WDFs in the LAB, where the parent particle X_2 move with speed β_2 , read

$$\mathcal{D}'_{\sigma'\lambda'}(\omega, \theta) = \sum_{\sigma'_2} \sum_{\sigma, \lambda} \sum_{\sigma_1} [d_{\sigma'\sigma}^{1/2}(\omega) d_{\lambda'\lambda}^{1/2}(\omega)] [d_{\sigma'_2, \sigma - \sigma_1}^{1/2}(\theta) d_{\sigma_2, \lambda - \sigma_1}^{1/2}(\theta)] F_{\sigma\sigma_1}^{1/2} F_{\lambda\sigma_1}^{1/2*}. \quad (\text{B.22})$$

For notational convenience, we introduce a parity-odd polarization parameter P_R and two parity-even polarization parameters, η_{1R} and η_{2R} , as

$$A = \frac{|F_{++}^{1/2}|^2 + |F_{+0}^{1/2}|^2 - |F_{--}^{1/2}|^2 - |F_{-0}^{1/2}|^2}{|F_{++}^{1/2}|^2 + |F_{+0}^{1/2}|^2 + |F_{--}^{1/2}|^2 + |F_{-0}^{1/2}|^2}, \quad (\text{B.23})$$

$$\eta_1 = \frac{|F_{++}^{1/2}|^2 - |F_{+0}^{1/2}|^2 + |F_{--}^{1/2}|^2 - |F_{-0}^{1/2}|^2}{|F_{++}^{1/2}|^2 + |F_{+0}^{1/2}|^2 + |F_{--}^{1/2}|^2 + |F_{-0}^{1/2}|^2}, \quad (\text{B.24})$$

$$\eta_2 = \frac{2\text{Re}(F_{+0}^{1/2} F_{-0}^{1/2*})}{|F_{++}^{1/2}|^2 + |F_{+0}^{1/2}|^2 + |F_{--}^{1/2}|^2 + |F_{-0}^{1/2}|^2}. \quad (\text{B.25})$$

In terms of the polarization parameters, A and $\eta_{1,2}$ we can derive two diagonal elements and thus the degree of longitudinal polarization P_L in the LAB as

$$\rho_{\pm\pm}^Y = \frac{1}{2} \left[1 \pm (\langle \cos \omega \rangle A - \langle \cos \omega \cos \theta \rangle P^{X_2} \eta_1 + \langle \sin \omega \sin \theta \rangle P^{X_2} \eta_2) \right], \quad (\text{B.26})$$

$$P_L = \langle \cos \omega \rangle A - \langle \cos \omega \cos \theta \rangle P^{X_2} \eta_1 + \langle \sin \omega \sin \theta \rangle P^{X_2} \eta_2. \quad (\text{B.27})$$

The two-body decay $T \rightarrow tZ$ of a new heavy top quark T into a top quark t and a Z in the little Higgs model is studied in detail as a characteristic example of this category in Subsection 5.3.

B.7 $1/2 \rightarrow 1 + 1/2$

This category contains several SM examples such as $t \rightarrow W^+ b$, $\tau^- \rightarrow \rho^- \nu_\tau$, and $\tau^- \rightarrow a^- \nu_\tau$ as well as the loop-induced flavor-changing processes such as $t \rightarrow Zc$.

In the X_2 rest frame, the helicity amplitude can be cast into the form:

$$D_{\sigma_2; \sigma, \sigma_1} = F_{\sigma\sigma_1}^{1/2} d_{\sigma_2, \sigma - \sigma_1}^{1/2}(\theta) e^{i\sigma_2 \phi}, \quad (\text{B.28})$$

where the X_2 helicity $\sigma_2 = \pm 1/2 = \pm$, the Y helicity $\sigma = \pm 1, 0 = \pm, 0$ and the X_1 helicity $\sigma_1 = \pm 1/2 = \pm$. Note that the amplitudes $F_{+-}^{1/2}$ and $F_{-+}^{1/2}$ are forbidden due to angular momentum conservation.

For notational convenience, let us introduce three parity-odd polarization parameters defined as

$$A_1 = \frac{|F_{++}^{1/2}|^2 - |F_{--}^{1/2}|^2}{|F_{++}^{1/2}|^2 + |F_{--}^{1/2}|^2 + |F_{0+}^{1/2}|^2 + |F_{0-}^{1/2}|^2}, \quad (\text{B.29})$$

$$A_2 = \frac{2\text{Re}(F_{++}^{1/2}F_{0+}^{1/2*} - F_{--}^{1/2}F_{0-}^{1/2*})}{|F_{++}^{1/2}|^2 + |F_{--}^{1/2}|^2 + |F_{0+}^{1/2}|^2 + |F_{0-}^{1/2}|^2}, \quad (\text{B.30})$$

$$A_3 = \frac{|F_{++}^{1/2}|^2 - |F_{--}^{1/2}|^2 + 2|F_{0+}^{1/2}|^2 - 2|F_{0-}^{1/2}|^2}{|F_{++}^{1/2}|^2 + |F_{--}^{1/2}|^2 + |F_{0+}^{1/2}|^2 + |F_{0-}^{1/2}|^2}, \quad (\text{B.31})$$

and two parity-even polarization parameters

$$\eta_1 = \frac{|F_{++}^{1/2}|^2 + |F_{--}^{1/2}|^2 - 2|F_{0+}^{1/2}|^2 - 2|F_{0-}^{1/2}|^2}{|F_{++}^{1/2}|^2 + |F_{--}^{1/2}|^2 + |F_{0+}^{1/2}|^2 + |F_{0-}^{1/2}|^2}, \quad (\text{B.32})$$

$$\eta_2 = \frac{2\text{Re}(F_{++}^{1/2}F_{0+}^{1/2*} + F_{--}^{1/2}F_{0-}^{1/2*})}{|F_{++}^{1/2}|^2 + |F_{--}^{1/2}|^2 + |F_{0+}^{1/2}|^2 + |F_{0-}^{1/2}|^2}. \quad (\text{B.33})$$

Three diagonal elements of the 3×3 density matrix ρ^Y averaged over the polar-angle distribution $d\Gamma/d\theta$ are given in terms of the five polarization parameters by

$$\begin{aligned} \rho_{\pm\pm}^Y &= \frac{1}{3} \pm \frac{1}{2} \langle \cos \omega \rangle A_1 + \frac{1}{12} \langle 3 \cos^2 \omega - 1 \rangle \eta_1 \\ &+ \frac{1}{2\sqrt{2}} \langle \cos \omega \sin \omega \sin \theta \rangle P^{X_2} A_2 + \frac{1}{12} \langle (3 \cos^2 \omega - 1) \cos \theta \rangle P^{X_2} A_3 \\ &\pm \frac{1}{6} \langle \cos \omega \cos \theta \rangle P^{X_2} (2 + \eta_1) \pm \frac{1}{2\sqrt{2}} \langle \sin \omega \sin \theta \rangle P^{X_2} \eta_2, \end{aligned} \quad (\text{B.34})$$

$$\begin{aligned} \rho_{00}^Y &= \frac{1}{3} - \frac{1}{6} \langle 3 \cos^2 \omega - 1 \rangle \eta_1 \\ &- \frac{1}{\sqrt{2}} \langle \cos \omega \sin \omega \sin \theta \rangle P^{X_2} A_2 - \frac{1}{6} \langle (3 \cos^2 \omega - 1) \cos \theta \rangle P^{X_2} A_3, \end{aligned} \quad (\text{B.35})$$

satisfying the normalization condition $\text{Tr}(\rho^Y) = \rho_{++}^Y + \rho_{00}^Y + \rho_{--}^Y = 1$.

B.8 $\boxed{1 \rightarrow 1/2 + 1/2}$

This decay category contains the SM processes such as the parity-violating weak decays of the massive weak bosons, $W^+ \rightarrow \tau^+ \nu_\tau$ and $Z \rightarrow \tau^- \tau^+$.

In the X_2 rest frame, the helicity amplitude of this type of decay modes can be cast into the form:

$$D_{\sigma_2; \sigma, \sigma_1} = F_{\sigma\sigma_1}^1 d_{\sigma_2, \sigma - \sigma_1}^1(\theta) e^{i\sigma_2 \phi}, \quad (\text{B.36})$$

where the X_2 helicity $\sigma_2 = \pm 1, 0 = \pm, 0$, the Y helicity $\sigma = \pm 1/2 = \pm$ and the X_1 helicity $\sigma_1 = \pm 1/2 = \pm$.

For notational convenience, let us introduce three parity-odd polarization parameters defined as

$$A_1 = \frac{|F_{++}^1|^2 - |F_{--}^1|^2 + |F_{+-}^1|^2 - |F_{-+}^1|^2}{|F_{++}^1|^2 + |F_{--}^1|^2 + |F_{+-}^1|^2 + |F_{-+}^1|^2}, \quad (\text{B.37})$$

$$A_2 = \frac{2\text{Re}(F_{++}^1 F_{-+}^{1*} - F_{--}^1 F_{+-}^{1*})}{|F_{++}^1|^2 + |F_{--}^1|^2 + |F_{+-}^1|^2 + |F_{-+}^1|^2}, \quad (\text{B.38})$$

$$A_3 = \frac{|F_{+-}^1|^2 - |F_{-+}^1|^2 - 2|F_{++}^1|^2 + 2|F_{--}^1|^2}{|F_{++}^1|^2 + |F_{--}^1|^2 + |F_{+-}^1|^2 + |F_{-+}^1|^2}, \quad (\text{B.39})$$

and two parity-even polarization parameters

$$\eta_1 = \frac{|F_{+-}^1|^2 + |F_{-+}^1|^2}{|F_{++}^1|^2 + |F_{--}^1|^2 + |F_{+-}^1|^2 + |F_{-+}^1|^2}, \quad (\text{B.40})$$

$$\eta_2 = \frac{2\text{Re}(F_{++}^1 F_{-+}^{1*} + F_{--}^1 F_{+-}^{1*})}{|F_{++}^1|^2 + |F_{--}^1|^2 + |F_{+-}^1|^2 + |F_{-+}^1|^2}. \quad (\text{B.41})$$

Two diagonal elements of the 2×2 density matrix ρ^Y averaged over the polar-angle distribution $d\Gamma/d\theta$ are given in terms of the five polarization parameters by

$$\begin{aligned} \rho_{\pm\pm}^Y &= \frac{1}{2} \pm \frac{1}{2} \langle \cos \omega \rangle A_1 \pm \frac{1}{8} \langle \cos \omega (3 \cos^2 \theta - 1) \rangle Q^{X_2} A_3 \\ &\pm \frac{3}{4} \langle \cos \omega \cos \theta \rangle P^{X_2} \eta_1 \pm \frac{3}{4\sqrt{2}} \langle \sin \omega \sin \theta \rangle P^{X_2} \eta_2 \\ &\mp \frac{3}{4\sqrt{2}} \langle \sin \omega \cos \theta \sin \theta \rangle Q^{X_2} A_2, \end{aligned} \quad (\text{B.42})$$

with the longitudinal polarization $P^{X_2} = \rho_{++}^{X_2} - \rho_{--}^{X_2}$ and the (diagonal) tensor polarization $Q^{X_2} = \rho_{++}^{X_2} + \rho_{--}^{X_2} - 2\rho_{00}^{X_2}$ of the decaying particle X_2 , satisfying the normalization condition $\text{Tr}(\rho^Y) = \rho_{++}^Y + \rho_{--}^Y = 1$.

B.9 1 \rightarrow 1 + 0

The process $Z \rightarrow W^\pm \pi^\mp$ in the SM might be an interesting example of this decay category, which is yet to be confirmed experimentally. A non-standard example is the decay of a heavy vector boson W_H^\pm into a SM gauge boson and a SM Higgs boson such as $W_H^\pm \rightarrow W^\pm H$, appearing in the little Higgs models [85].

In the X_2 rest frame, the helicity amplitude of this type of decay modes can be cast into the form:

$$D_{\sigma_2; \sigma} = F_{\sigma\sigma_1}^1 d_{\sigma_2, \sigma}^1(\theta) e^{i\sigma_2\phi}, \quad (\text{B.43})$$

where the X_2 helicity $\sigma_2 = \pm 1, 0 = \pm, 0$, the Y helicity $\sigma = \pm 1, 0 = \pm, 0$ while the X_1 particle is spinless.

For notational convenience, let us introduce two parity-odd polarization parameters defined as

$$A_1 = \frac{|F_+^1|^2 - |F_-^1|^2}{|F_+^1|^2 + |F_0^1|^2 + |F_-^1|^2}, \quad (\text{B.44})$$

$$A_2 = \frac{2\text{Re}(F_+^1 F_0^{1*} - F_-^1 F_0^{1*})}{|F_+^1|^2 + |F_0^1|^2 + |F_-^1|^2}, \quad (\text{B.45})$$

and three parity-even polarization parameters

$$\eta_1 = \frac{|F_+^1|^2 - 2|F_0^1|^2 + |F_-^1|^2}{|F_+^1|^2 + |F_0^1|^2 + |F_-^1|^2}, \quad (\text{B.46})$$

$$\eta_2 = \frac{2\text{Re}(F_+^1 F_0^{1*} + F_-^1 F_0^{1*})}{|F_+^1|^2 + |F_0^1|^2 + |F_-^1|^2}, \quad (\text{B.47})$$

$$\eta_3 = \frac{2\text{Re}(F_+^1 F_-^{1*})}{|F_+^1|^2 + |F_0^1|^2 + |F_-^1|^2}. \quad (\text{B.48})$$

The longitudinal (00) element of the 3×3 density matrix ρ^Y averaged over the polar-angle distribution is given in terms of the five polarization parameters by

$$\begin{aligned} \rho_{00}^Y &= \frac{1}{3} - \frac{1}{6} Q^{X_2} \eta_3 - \frac{1}{12} (3 \cos^2 \omega - 1) (2\eta_1 - Q^{X_2} \eta_3) \\ &\quad - \frac{1}{24} \langle (3 \cos^2 \omega - 1) (3 \cos^2 \theta - 1) \rangle Q^{X_2} (2 - \eta_1 + \eta_3) \\ &\quad - \frac{3}{4} \langle \cos \omega \sin \omega \cos \theta \sin \theta \rangle Q^{X_2} \eta_2 \\ &\quad - \frac{1}{4} \langle (3 \cos^2 \omega - 1) \cos \theta \rangle P^{X_2} A_1 - \frac{3}{4} \langle \cos \omega \sin \omega \sin \theta \rangle P^{X_2} A_2, \end{aligned} \quad (\text{B.49})$$

and two transverse elements of the density matrix by

$$\rho_{\pm\pm}^Y = \frac{1}{2} (\rho_T^Y \pm \rho_T'^Y), \quad (\text{B.50})$$

with the sum and difference, ρ^Y and $\rho_T'^Y$, defined as

$$\begin{aligned} \rho_T^Y &= \frac{2}{3} + \frac{1}{6} Q^{X_2} \eta_3 + \frac{1}{12} (3 \cos^2 \omega - 1) (2\eta_R - Q^{X_2} \eta_3) \\ &\quad + \frac{1}{24} \langle (3 \cos^2 \omega - 1) (3 \cos^2 \theta - 1) \rangle Q^{X_2} (2 - \eta_1 + \eta_3) \\ &\quad + \frac{3}{4} \langle \cos \omega \sin \omega \cos \theta \sin \theta \rangle Q^{X_2} \eta_2 \\ &\quad + \frac{1}{4} \langle (3 \cos^2 \omega - 1) \cos \theta \rangle P^{X_2} A_1 + \frac{3}{4} \langle \cos \omega \sin \omega \sin \theta \rangle P^{X_2} A_2, \end{aligned} \quad (\text{B.51})$$

$$\begin{aligned} \rho_T'^Y &= \langle \cos \omega \rangle A_1 + \frac{1}{2} \langle \cos \omega \cos \theta \rangle P^{X_2} (2 + \eta_1) \\ &\quad + \frac{3}{4} \langle \sin \omega \sin \theta \rangle P^{X_2} \eta_2 \\ &\quad + \frac{1}{4} \langle \cos \omega (3 \cos^2 \theta - 1) \rangle Q^{X_2} A_1 + \frac{3}{4} \langle \sin \omega \cos \theta \sin \theta \rangle Q^{X_2} A_2, \end{aligned} \quad (\text{B.52})$$

with the longitudinal polarization $P^{X_2} = \rho_{++}^{X_2} - \rho_{--}^{X_2}$ and the (diagonal) tensor polarization $Q^{X_2} = \rho_{++}^{X_2} - 2\rho_{00}^{X_2} + \rho_{--}^{X_2}$ of the decaying particle X_2 , satisfying the normalization condition $\text{Tr}(\rho^Y) = \rho_T^Y + \rho_{00}^Y = 1$.

B.10 1 \rightarrow 1 + 1

The process $Z \rightarrow W^\pm \rho^\mp$ might be an example of this decay category, which is yet to be confirmed experimentally. A non-standard example is the decay of a heavy vector boson W_H^\pm into two SM gauge bosons such as $W_H^\pm \rightarrow W^\pm Z$, appearing in the little Higgs models [85]

In the X_2 rest frame, the helicity amplitude of this type of decay modes can be cast into the form:

$$D_{\sigma_2; \sigma, \sigma_1} = F_{\sigma\sigma_1}^1 d_{\sigma_2, \sigma - \sigma_1}^1(\theta) e^{i\sigma_2\phi}, \quad (\text{B.53})$$

where the X_2 helicity $\sigma_2 = \pm 1, 0 = \pm, 0$, the Y helicity $\sigma = \pm 1, 0 = \pm, 0$ while the X_1 particle is spinless.

For notational convenience, we introduce the full sum of absolute squares of reduces helicity amplitudes Σ_{11}^1

$$\Sigma_{11}^1 = |F_{++}^1|^2 + |F_{10}^1|^2 + |F_{01}^1|^2 + |F_{00}^1|^2 + |F_{0-}^1|^2 + |F_{-0}^1|^2 + |F_{--}^1|^2, \quad (\text{B.54})$$

as well as five parity-odd polarization parameters defined as

$$A_1 = \frac{|F_{+0}^1|^2 - |F_{-0}^1|^2 + 2|F_{0+}^1|^2 - 2|F_{0-}^1|^2}{\Sigma_{11}^1}, \quad (\text{B.55})$$

$$A_2 = \frac{|F_{++}^1|^2 - |F_{--}^1|^2 + |F_{+0}^1|^2 - |F_{-0}^1|^2}{\Sigma_{11}^1}, \quad (\text{B.56})$$

$$A_3 = \frac{2|F_{++}^1|^2 - 2|F_{--}^1|^2 - |F_{+0}^1|^2 + |F_{-0}^1|^2}{\Sigma_{11}^1}, \quad (\text{B.57})$$

$$A_4 = \frac{2\text{Re}(F_{++}^1 F_{0+}^{1*} - F_{--}^1 F_{0-}^{1*} + F_{+0}^1 F_{00}^{1*} - F_{-0}^1 F_{00}^{1*})}{\Sigma_{11}^1}, \quad (\text{B.58})$$

$$A_5 = \frac{2\text{Re}(F_{++}^1 F_{0+}^{1*} - F_{--}^1 F_{0-}^{1*} - F_{+0}^1 F_{00}^{1*} + F_{-0}^1 F_{00}^{1*})}{\Sigma_{11}^1}, \quad (\text{B.59})$$

and six parity-even polarization parameters

$$\eta_1 = \frac{|F_{++}^1|^2 + |F_{--}^1|^2 + |F_{+0}^1|^2 + |F_{-0}^1|^2 - 2|F_{0+}^1|^2 - 2|F_{00}^1|^2 - 2|F_{0-}^1|^2}{\Sigma_{11}^1}, \quad (\text{B.60})$$

$$\eta_2 = \frac{|F_{+0}^1|^2 - 2|F_{00}^1|^2 + 2|F_{-0}^1|^2}{\Sigma_{11}^1}, \quad (\text{B.61})$$

$$\eta_3 = \frac{|F_{++}^1|^2 + |F_{0+}^1|^2 + |F_{0-}^1|^2 + |F_{--}^1|^2}{\Sigma_{11}^1}, \quad (\text{B.62})$$

$$\eta_4 = \frac{2\text{Re}(F_{++}^1 F_{0+}^{1*} + F_{--}^1 F_{0-}^{1*} - F_{+0}^1 F_{00}^{1*} - F_{-0}^1 F_{00}^{1*})}{\Sigma_{11}^1}, \quad (\text{B.63})$$

$$\eta_5 = \frac{2\text{Re}(F_{++}^1 F_{0+}^{1*} + F_{--}^1 F_{0-}^{1*} + F_{+0}^1 F_{00}^{1*} + F_{-0}^1 F_{00}^{1*})}{\Sigma_{11}^1}, \quad (\text{B.64})$$

$$\eta_6 = \frac{2\text{Re}(F_{+0}^1 F_{-0}^{1*})}{\Sigma_{11}^1}. \quad (\text{B.65})$$

The longitudinal (00) element of the 3×3 density matrix ρ^Y averaged over the polar-angle distribution is given in terms of the six polarization parameters by

$$\begin{aligned} \rho_{00}^Y &= \rho_L^Y = \frac{1}{3} - \frac{1}{6} Q^{X_2} \eta_6 - \frac{1}{12} \langle 3 \cos^2 \omega - 1 \rangle (2\eta_1 - Q^{X_2} \eta_6) - \frac{1}{4} \langle (3 \cos^2 \omega - 1) \cos \theta \rangle P^{X_2} A_1 \\ &\quad - \frac{3}{4} \langle \sin \omega \cos \omega \sin \theta \rangle P^{X_2} A_4 + \frac{1}{24} \langle (3 \cos^2 \omega - 1) (3 \cos^2 \theta - 1) \rangle Q^{X_2} (4\eta_3 - 2 + \eta_2 - \eta_6) \\ &\quad + \frac{3}{4} \langle \cos \omega \sin \omega \cos \theta \sin \theta \rangle Q^{X_2} \eta_4, \end{aligned} \quad (\text{B.66})$$

and two transverse elements of the density matrix by

$$\rho_{\pm\pm}^Y = \frac{1}{2}(\rho_T^Y \pm \rho_T'^Y), \quad (\text{B.67})$$

with the sum ρ^Y and the difference $\rho_T'^Y$ defined as

$$\begin{aligned} \rho_T^Y &= \frac{2}{3} + \frac{1}{6}Q^{X_2}\eta_6 + \frac{1}{12}\langle 3\cos^2\omega - 1 \rangle(2\eta_1 - Q^{X_2}\eta_6) - \frac{1}{4}\langle (3\cos^2\omega - 1)\cos\theta \rangle P^{X_2}A_1 \\ &\quad + \frac{3}{4}\langle \sin\omega\cos\omega\sin\theta \rangle P^{X_2}A_4 - \frac{1}{24}\langle (3\cos^2\omega - 1)(3\cos^2\theta - 1) \rangle Q^{X_2}(4\eta_3 - 2 + \eta_2 - \eta_6) \\ &\quad - \frac{3}{4}\langle \cos\omega\sin\omega\cos\theta\sin\theta \rangle Q^{X_2}\eta_4, \end{aligned} \quad (\text{B.68})$$

$$\begin{aligned} \rho_T'^Y &= \langle \cos\omega \rangle A_2 + \frac{1}{2}\langle \cos\omega\cos\theta \rangle P^{X_2}(2 + \eta_2 - 2\eta_3) + \frac{3}{4}\langle \sin\omega\sin\theta \rangle P^{X_2}\eta_5 \\ &\quad - \frac{1}{4}\langle \cos\omega(3\cos^2\theta - 1) \rangle Q^{X_2}A_3 - \frac{3}{4}\langle \sin\omega\cos\theta\sin\theta \rangle Q^{X_2}A_5, \end{aligned} \quad (\text{B.69})$$

with the longitudinal polarization $P^{X_2} = \rho_{++}^{X_2} - \rho_{--}^{X_2}$ and the (diagonal) tensor polarization $Q^{X_2} = \rho_{++}^{X_2} - 2\rho_{00}^{X_2} + \rho_{--}^{X_2}$ of the decaying particle X_2 , satisfying the normalization condition $\text{Tr}(\rho^Y) = \rho_T^Y + \rho_{00}^Y = 1$.

C Polarization estimator functions

In this appendix, we exhibit all the essential functions defining the averages of the polar-angle correlations over the polar angle θ of the products, which consist of trigonometric functions of ω and θ explicitly in terms of β_2 and β . We call them *polarization estimator functions*, reflecting the naming *polarization estimators* in Refs. [39, 40].

For notational convenience and for the sake of discussion let us introduce the following combinations of two speed parameters β_2 and β as⁷

$$\beta_+ = \frac{1}{2}(\beta_2 + \beta + |\beta_2 - \beta|) = \max(\beta_2, \beta), \quad (\text{C.70})$$

$$\beta_- = \frac{1}{2}(\beta_2 + \beta - |\beta_2 - \beta|) = \min(\beta_2, \beta), \quad (\text{C.71})$$

and three auxiliary functions of β_2 and β defined by

$$\mathcal{L}_1(\beta_2, \beta) = \frac{1}{\beta_2\beta^2}\beta_- - \frac{(1 - \beta^2)}{2\beta_2\beta^2} \ln\left(\frac{1 + \beta_-}{1 - \beta_-}\right), \quad (\text{C.72})$$

and

$$\mathcal{L}_2(\beta_2, \beta) = \begin{cases} \frac{1}{\beta_2\beta} \ln\left|\frac{\beta_2 + \beta}{\beta_2 - \beta}\right| - \gamma_2\gamma \frac{(2 - \beta_2^2 - \beta^2)}{2\beta_2\beta} \ln\left|\frac{\gamma_2\beta_2 + \gamma\beta}{\gamma_2\beta_2 - \gamma\beta}\right| & \text{for } \beta_2 \neq \beta, \\ -\frac{1}{\beta^2} \ln(1 - \beta^2) & \text{for } \beta_2 = \beta, \end{cases} \quad (\text{C.73})$$

$$\mathcal{L}_3(\beta_2, \beta) = \begin{cases} \frac{(4 - \beta_2^2 - \beta^2)}{2\beta_2\beta} \ln\left|\frac{\beta_2 + \beta}{\beta_2 - \beta}\right| - \gamma_2\gamma \frac{(4 - 3\beta_2^2 - 3\beta^2 + 2\beta_2^2\beta^2)}{2\beta_2\beta} \ln\left|\frac{\gamma_2\beta_2 + \gamma\beta}{\gamma_2\beta_2 - \gamma\beta}\right| & \text{for } \beta_2 \neq \beta, \\ -\frac{(2 - \beta^2)}{\beta^2} \ln(1 - \beta^2) & \text{for } \beta_2 = \beta, \end{cases} \quad (\text{C.74})$$

⁷It is interesting to note that the n -th power of β_{\pm} is simply $\beta_{\pm}^n = \frac{1}{2}(\beta_2^n + \beta^n \pm |\beta_2^n - \beta^n|)$ for an arbitrary integer n .

Polarization estimator functions	$\beta_2 \rightarrow 1$	$\beta_2 = 0$ or $\beta = 1$
$\langle \cos \omega \rangle$	$\mathcal{L}_1(1, \beta)$	1
$\langle \cos \omega \cos \theta \rangle$	$1 - \mathcal{L}_1(\beta, \beta)$	0
$\langle \cos \omega \cos^2 \theta \rangle$	$\frac{1}{\beta} [\mathcal{L}_1(\beta, \beta) - 2/3]$	$\frac{1}{3}$
$\langle \sin \omega \sin \theta \rangle$	$\sqrt{1 - \beta^2} \mathcal{L}_1(\beta, \beta)$	0
$\langle \sin \omega \cos \theta \sin \theta \rangle$	$\frac{\sqrt{1 - \beta^2}}{\beta} [2/3 - \mathcal{L}_1(\beta, \beta)]$	0
$\langle \cos^2 \omega \rangle$	$2\mathcal{L}_1(\beta, \beta) - 1$	1
$\langle \cos^2 \omega \cos \theta \rangle$	$\frac{1}{\beta} [2 - (3 - \beta^2) \mathcal{L}_1(\beta, \beta)]$	0
$\langle \cos^2 \omega \cos^2 \theta \rangle$	$\frac{1}{\beta^2} [\beta^2 - 8/3 + 2(2 - \beta^2) \mathcal{L}_1(\beta, \beta)]$	$\frac{1}{3}$
$\langle \cos \omega \sin \omega \sin \theta \rangle$	$\frac{\sqrt{1 - \beta^2}}{\beta} [3 \mathcal{L}_1(\beta, \beta) - 2]$	0
$\langle \cos \omega \sin \omega \cos \theta \sin \theta \rangle$	$\frac{\sqrt{1 - \beta^2}}{\beta^2} [8/3 - (4 - \beta^2) \mathcal{L}_1(\beta, \beta)]$	0

Table 3: Asymptotic expressions of ten polarization estimators to be valid when $\beta_2 \rightarrow 1$, i.e. the decaying particle X_2 is highly relativistic and so greatly energetic. In addition, the last column shows the trivial values for $\beta_2 = 0$ or $\beta = 1$ for which no Wick helicity rotation is developed.

with the X_2 and Y boost factors $\gamma_2 = 1/\sqrt{1 - \beta_2^2}$ and $\gamma = 1/\sqrt{1 - \beta^2}$. Folding these functions with proper ratios of polynomial functions enable us to express all the polarization estimator functions in terms of β_2 and β .

In order to avoid the apparently-looking singular structure in $\mathcal{L}_{2,3}(\beta_2, \beta)$ with $\beta_2 = \beta$ in Eqs. (C.74) and (C.74), it is worthwhile to reexpress the functions in a good singular-free form as

$$\mathcal{L}_2(\beta_2, \beta) = \mathcal{L}_+(\beta_2, \beta) - \mathcal{L}_-(\beta_2, \beta), \quad (\text{C.75})$$

$$\mathcal{L}_3(\beta_2, \beta) = \frac{1}{\gamma_2 \gamma} [(\gamma_2 \gamma + 1) \mathcal{L}_+(\beta_2, \beta) - (\gamma_2 \gamma - 1) \mathcal{L}_-(\beta_2, \beta)], \quad (\text{C.76})$$

in terms of the following two logarithmic functions:

$$\mathcal{L}_{\pm}(\beta_2, \beta) = \frac{(\gamma_2 \pm \gamma)^2}{4\gamma_2 \beta_2 \gamma \beta} \ln \left(\frac{\gamma_2 \gamma + \gamma_2 \beta_2 \gamma \beta \pm 1}{\gamma_2 \gamma - \gamma_2 \beta_2 \gamma \beta \pm 1} \right). \quad (\text{C.77})$$

For $\beta_2 = \beta$, we have a compact expression of $\mathcal{L}_+(\beta, \beta) = -\ln(1 - \beta^2)/\beta^2$ and $\mathcal{L}_-(\beta, \beta) = 0$ with the limit $\mathcal{L}_+(0, 0) = 1$, free from any apparent singularities.

As noted before, no Wick helicity rotation is developed when $\beta_2 = 0$ or $\beta = 1$, i.e. $\omega = 0$, leading to trivial values of the polarization estimators.⁸ In contrast, the polarization estimator functions have their non-trivial limits as $\beta_2 \rightarrow 1$.

⁸It is unnecessary to consider the limit of $\beta = 0$ as the process $X_2 \rightarrow YX_1$ will not occur due to the vanishing phase space for the production of Y and X_1 at rest.

It is a trivial observation that there is no Wick helicity rotation, if the particle Y is spinless, i.e. $j = 0$. On the other hand, if the decaying particle X_2 is spinless with $j_2 = 0$, only two polarization estimators $\langle \cos \omega \rangle$ and $\langle \cos^2 \omega \rangle$ appear in the decay $X_2 \rightarrow YX_1$ for $j = 1/2$ and $j = 1$, as the decay angular distribution in the X_2 rest frame is isotropic, i.e. a constant. The former estimator function $\langle \cos \omega \rangle$ is involved in the final-state mode $\|\frac{1}{2}1\|$ and/or mode $\|11\|$, if parity is violated in the decay, and the latter estimator function $\langle \cos^2 \omega \rangle$ appears in the final-state modes $\|10\|$ and $\|11\|$ with a spin-1 Y . Explicitly, they can be written in terms of the functions $\mathcal{L}_{1,2,3}$ as

$$\langle \cos \omega \rangle = \mathcal{L}_1(\beta_2, \beta), \quad (\text{C.78})$$

$$\langle \cos^2 \omega \rangle = \frac{1}{\beta^2} [1 - (1 - \beta^2) \mathcal{L}_2(\beta_2, \beta)], \quad (\text{C.79})$$

where β_2 and β are the speeds of X_2 in the LAB and Y in the X_2 rest frame, respectively. Their asymptotic expressions in the limit $\beta_2 \rightarrow 1$ are listed in the second and third rows of Table 3.

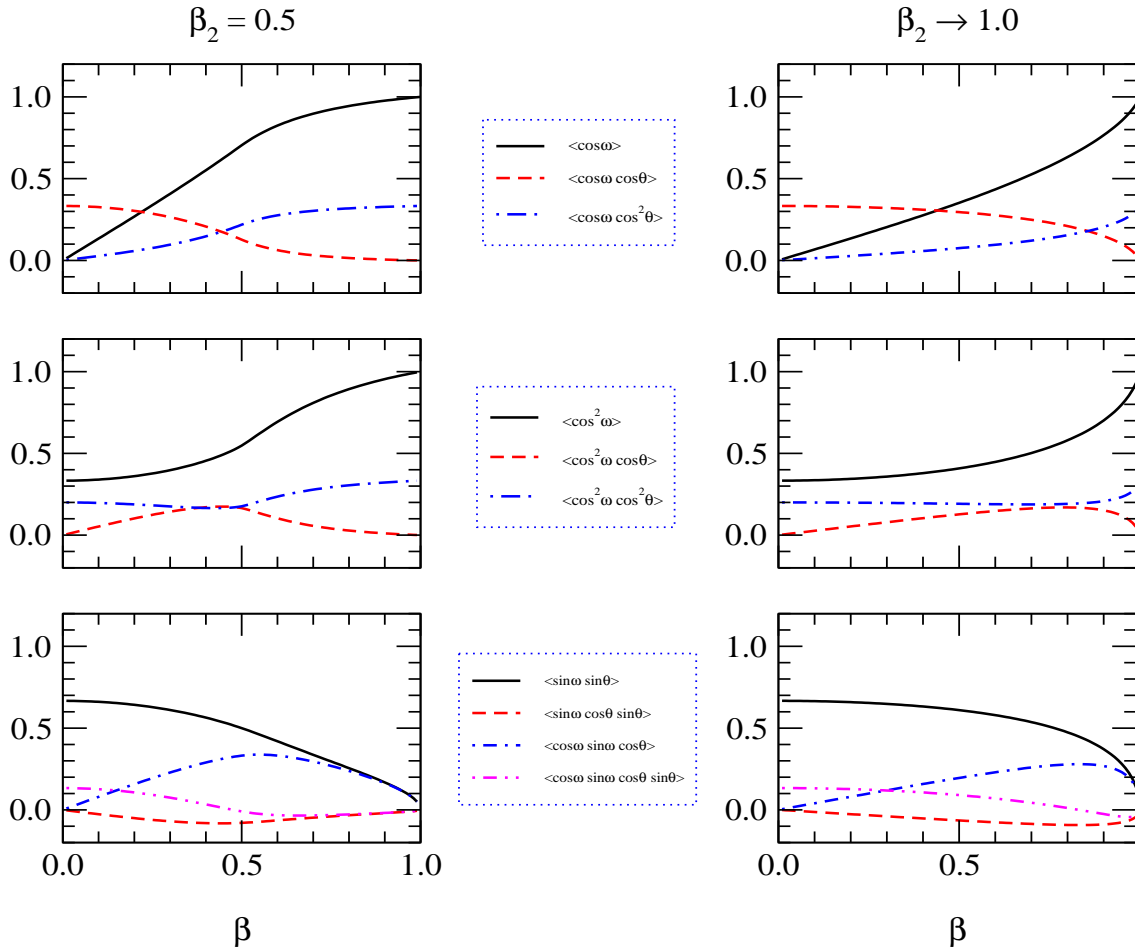


Figure 8: The β dependence of ten polarization estimators for fixed $\beta_2 = 0.5$ (left) and as $\beta_2 \rightarrow 1.0$ (right). Note that there exists a rather abrupt slope change near $\beta = \beta_2$ as indicated clearly by the lines on the left panel.

If the particle X_2 of non-zero spin carries non-zero polarization in a production process of X_2 production,

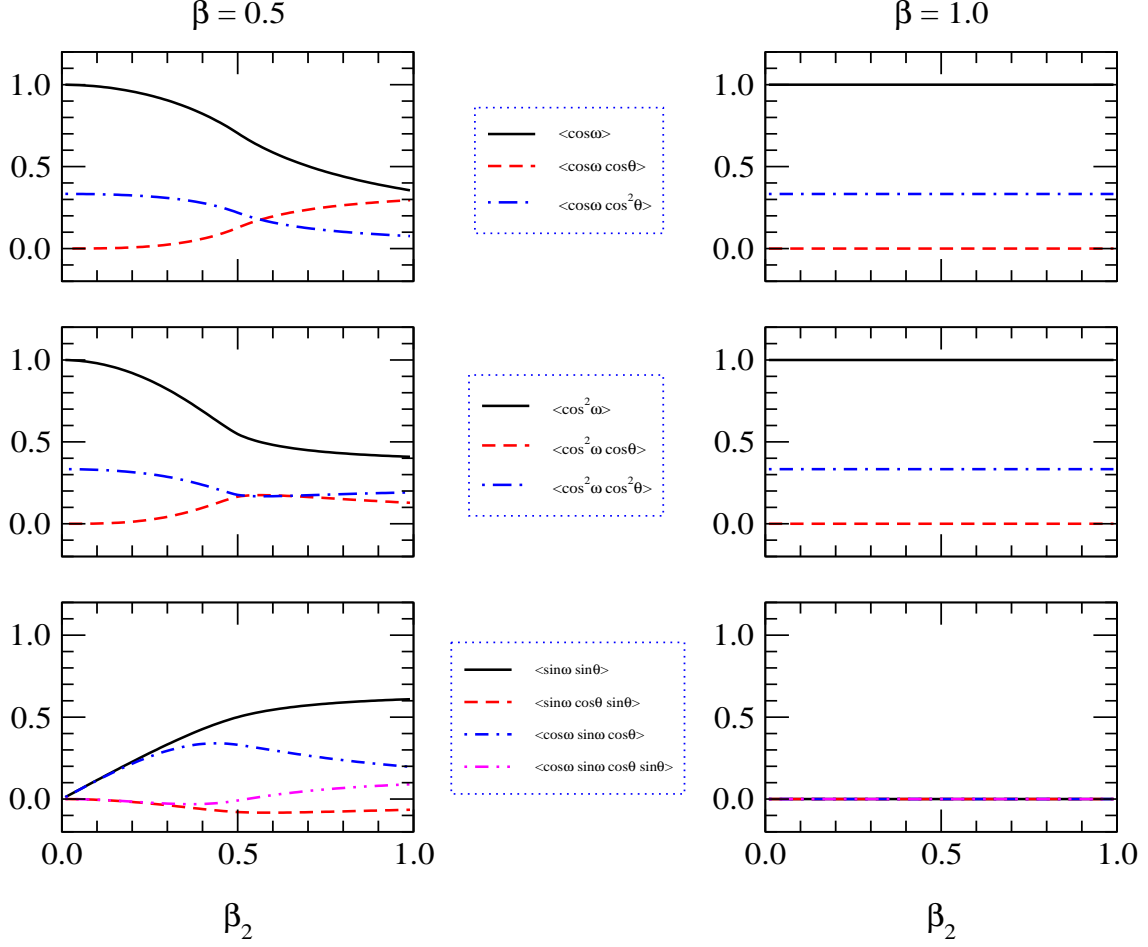


Figure 9: The β_2 dependence of ten polarization estimators for $\beta = 0.5$ (left) and $\beta = 1.0$ (right). As mentioned in the main text, there is no Wick helicity rotation for $\beta = 1.0$ with a massless Y , reflected clearly by the fact that all the polarization estimators are constant in β_2 .

non-trivial Wick helicity rotation effects are developed for a non-zero spin j of the particle Y . Besides two estimators $\langle \cos \omega \rangle$ and $\langle \cos^2 \omega \rangle$, there are eight additional non-trivial polarization estimators, involving the sines and cosines of not only ω but also of θ explicitly. The non-trivial functions in β_2 and β can be classified into, firstly, two $\cos \omega$ -involved functions

$$\langle \cos \omega \cos \theta \rangle = \frac{1}{2\beta_2\beta} \left[\frac{1}{\beta} \beta_+ - \frac{(\beta_2^2 - 2\beta^2)}{\beta_2\beta^2} \beta_- - (3 - \beta_2^2) \mathcal{L}_1(\beta_2, \beta) \right], \quad (\text{C.80})$$

$$\langle \cos \omega \cos^2 \theta \rangle = -\frac{1}{2\beta_2^2\beta^2} \left[\frac{(5 - 3\beta^2)}{3\beta} \beta_+ - \frac{(5\beta_2^2 - 10\beta^2 + 3\beta_2^2\beta^2)}{3\beta_2\beta^2} \beta_- - (5 - 3\beta_2^2 - \beta^2 + \beta_2^2\beta^2) \mathcal{L}_1(\beta_2, \beta) \right], \quad (\text{C.81})$$

secondly, two $\sin \omega$ -involved functions expressed in terms of the logarithmic function $\mathcal{L}_1(\beta_2, \beta)$ as

$$\langle \sin \omega \sin \theta \rangle = -\frac{\gamma}{2\beta_2\beta} \left[\frac{(1-\beta^2)}{\beta} \beta_+ - \frac{(\beta_2^2 - 2\beta^2 + \beta_2^2\beta^2)}{\beta_2\beta^2} \beta_- - (3 - \beta_2^2 - \beta^2 - \beta_2^2\beta^2) \mathcal{L}_1(\beta_2, \beta) \right], \quad (\text{C.82})$$

$$\langle \sin \omega \cos \theta \sin \theta \rangle = \frac{\gamma}{2\beta_2^2\beta^2} \left[\frac{5(1-\beta^2)}{3\beta} \beta_+ - \frac{(5\beta_2^2 - 10\beta^2 + \beta_2^2\beta^2 + 4\beta^4)}{3\beta_2\beta^2} \beta_- - (5 - 3\beta_2^2 - 3\beta^2 + \beta_2^2\beta^2) \mathcal{L}_1(\beta_2, \beta) \right], \quad (\text{C.83})$$

thirdly, two $\cos^2 \omega$ -involved functions expressed in terms of two logarithmic functions $\mathcal{L}_{2,3}(\beta_2, \beta)$ as

$$\langle \cos^2 \omega \cos \theta \rangle = -\frac{(1-\beta^2)}{\beta_2\beta^3} [2 - \mathcal{L}_3(\beta_2, \beta)], \quad (\text{C.84})$$

$$\langle \cos^2 \omega \cos^2 \theta \rangle = \frac{1}{3\beta^2} + \frac{1}{\beta_2^2\gamma^2\beta^4} [4 - \beta_2^2 - \beta^2 + (\beta_2^2 + \beta^2 - \beta_2^2\beta^2) \mathcal{L}_2(\beta_2, \beta) - 2\mathcal{L}_3(\beta_2, \beta)], \quad (\text{C.85})$$

and finally two $(\cos \omega \sin \omega)$ -involved functions expressed in terms of the logarithmic functions $\mathcal{L}_{2,3}(\beta_2, \beta)$ as

$$\langle \cos \omega \sin \omega \sin \theta \rangle = \frac{1}{\beta_2\gamma\beta^3} [2 - \beta^2 + \beta^2 \mathcal{L}_2(\beta_2, \beta) - \mathcal{L}_3(\beta_2, \beta)], \quad (\text{C.86})$$

$$\langle \cos \omega \sin \omega \cos \theta \sin \theta \rangle = -\frac{1}{\beta_2^2\gamma\beta^4} \left[4 - \beta_2^2 - 3\beta^2 + \frac{1}{3}\beta_2^2\beta^2 + (\beta_2^2 + \beta^2 - \beta_2^2\beta^2) \mathcal{L}_2(\beta_2, \beta) - (2 - \beta^2) \mathcal{L}_3(\beta_2, \beta) \right], \quad (\text{C.87})$$

where β_2 and β are the X_2 speed in the LAB and the Y speed in the X_2 rest frame and $\gamma_2 = 1/\sqrt{1-\beta^2}$ and $\gamma = 1/\sqrt{1-\beta_2^2}$, respectively.

The asymptotic expressions of the polarization estimator functions when $\beta_2 \rightarrow 1$, i.e. the particle X_2 is highly relativistic are listed in the second column of Table 3. In addition, for the sake of reference, we list the values for $\beta_2 = 0$ and/or $\beta = 1$ in the third column of the table that are trivially constant because of no Wick helicity rotation in those limits.

References

- [1] E. P. Wigner, “On Unitary Representations of the Inhomogeneous Lorentz Group,” *Annals Math.* **40** (1939) 149 [*Nucl. Phys. Proc. Suppl.* **6** (1989) 9].
- [2] C. Bourrely, J. Soffer and E. Leader, “Polarization Phenomena in Hadronic Reactions,” *Phys. Rept.* **59** (1980) 95.
- [3] C. Bourrely, J. Soffer, F. M. Renard and P. Taxil, “Spin Effects At Supercollider Energies,” *Phys. Rept.* **177** (1989) 319.
- [4] E. Leader, “Spin in particle physics,” *Camb. Monogr. Part. Phys. Nucl. Phys. Cosmol.* **15** (2011) 500 p.

- [5] L. Evans and P. Bryant, “LHC Machine,” JINST **3** (2008) S08001.
- [6] G. Aad *et al.* [ATLAS Collaboration], “Observation of a new particle in the search for the Standard Model Higgs boson with the ATLAS detector at the LHC,” Phys. Lett. B **716** (2012) 1 [arXiv:1207.7214 [hep-ex]].
- [7] S. Chatrchyan *et al.* [CMS Collaboration], “Observation of a new boson at a mass of 125 GeV with the CMS experiment at the LHC,” Phys. Lett. B **716** (2012) 30 [arXiv:1207.7235 [hep-ex]].
- [8] G. Aad *et al.* [ATLAS and CMS Collaborations], “Combined Measurement of the Higgs Boson Mass in pp Collisions at $\sqrt{s} = 7$ and 8 TeV with the ATLAS and CMS Experiments,” Phys. Rev. Lett. **114** (2015) 191803 [arXiv:1503.07589 [hep-ex]].
- [9] G. Aad *et al.* [ATLAS and CMS Collaborations], “Measurements of the Higgs boson production and decay rates and constraints on its couplings from a combined ATLAS and CMS analysis of the LHC pp collision data at $\sqrt{s} = 7$ and 8 TeV,” JHEP **1608** (2016) 045 [arXiv:1606.02266 [hep-ex]].
- [10] S. Y. Choi, D. J. Miller, M. M. Muhlleitner and P. M. Zerwas, “Identifying the Higgs spin and parity in decays to Z pairs,” Phys. Lett. B **553** (2003) 61 [hep-ph/0210077].
- [11] Y. Gao, A. V. Gritsan, Z. Guo, K. Melnikov, M. Schulze and N. V. Tran, “Spin determination of single-produced resonances at hadron colliders,” Phys. Rev. D **81** (2010) 075022 [arXiv:1001.3396 [hep-ph]].
- [12] A. De Rujula, J. Lykken, M. Pierini, C. Rogan and M. Spiropulu, “Higgs look-alikes at the LHC,” Phys. Rev. D **82** (2010) 013003 [arXiv:1001.5300 [hep-ph]].
- [13] S. Bolognesi, Y. Gao, A. V. Gritsan, K. Melnikov, M. Schulze, N. V. Tran and A. Whitbeck, “On the spin and parity of a single-produced resonance at the LHC,” Phys. Rev. D **86** (2012) 095031 [arXiv:1208.4018 [hep-ph]].
- [14] G. Aad *et al.* [ATLAS Collaboration], “Study of the spin and parity of the Higgs boson in diboson decays with the ATLAS detector,” Eur. Phys. J. C **75** (2015) no.10, 476 Erratum: [Eur. Phys. J. C **76** (2016) no.3, 152] [arXiv:1506.05669 [hep-ex]].
- [15] V. Khachatryan *et al.* [CMS Collaboration], “Constraints on the spin-parity and anomalous HVV couplings of the Higgs boson in proton collisions at 7 and 8 TeV,” Phys. Rev. D **92** (2015) no.1, 012004 [arXiv:1411.3441 [hep-ex]].
- [16] S. Weinberg, “Implications of dynamical symmetry breaking,” Phys. Rev. D **13**, 974 (1976).
- [17] S. Weinberg, “Implications Of Dynamical Symmetry Breaking: An Addendum,” Phys. Rev. D **19**, 1277 (1979).
- [18] L. Susskind, “Dynamics of spontaneous symmetry breaking in the Weinberg-Salam theory,” Phys. Rev. D **20**, 2619 (1979).
- [19] G. ’t Hooft, in *Recent developments in gauge theories*, Proceedings of the NATO Advanced Summer Institute, Cargese 1979, ed. G. ’t Hooft *et al.* (Plenum, New York 1980).
- [20] H. P. Nilles, “Supersymmetry, Supergravity And Particle Physics,” Phys. Rept. **110**, 1 (1984).
- [21] H. E. Haber and G. L. Kane, “The Search for Supersymmetry: Probing Physics Beyond the Standard Model,” Phys. Rept. **117** (1985) 75.
- [22] D. J. H. Chung, L. L. Everett, G. L. Kane, S. F. King, J. D. Lykken and L. T. Wang, “The soft supersymmetry-breaking Lagrangian: Theory and applications,” Phys. Rept. **407**, 1 (2005) [arXiv:hep-ph/0312378].

- [23] M. Drees, R. Godbole and P. Roy, “Theory and phenomenology of sparticles: An account of four-dimensional $N = 1$ supersymmetry in high energy physics,” Hackensack, USA: World Scientific (2004) 555 p.
- [24] P. Binetruy, “Supersymmetry: Theory, experiment and cosmology,” Oxford, UK: Oxford Univ. Pr. (2006) 520 p.
- [25] J. Wess and J. Bagger, “Supersymmetry and supergravity,” Princeton, USA: Univ. Pr. (1992) 259 p.
- [26] T. Appelquist, H. C. Cheng and B. A. Dobrescu, “Bounds on universal extra dimensions,” Phys. Rev. D **64**, 035002 (2001) [arXiv:hep-ph/0012100].
- [27] T. Kakuda, K. Nishiwaki, K. y. Oda and R. Watanabe, “Universal extra dimensions after Higgs discovery,” Phys. Rev. D **88** (2013) 035007 [arXiv:1305.1686 [hep-ph]].
- [28] F. Boudjema and R. K. Singh, “A Model independent spin analysis of fundamental particles using azimuthal asymmetries,” JHEP **0907** (2009) 028 [arXiv:0903.4705 [hep-ph]].
- [29] A. J. Barr, “Determining the spin of supersymmetric particles at the LHC using lepton charge asymmetry,” Phys. Lett. B **596** (2004) 205 [hep-ph/0405052].
- [30] A. J. Barr, JHEP **0602**, 042 (2006) [arXiv:hep-ph/0511115].
- [31] J. M. Smillie and B. R. Webber, “Distinguishing spins in supersymmetric and universal extra dimension models at the Large Hadron Collider,” JHEP **0510**, 069 (2005) [arXiv:hep-ph/0507170].
- [32] L. T. Wang and I. Yavin, “Spin measurements in cascade decays at the LHC,” JHEP **0704** (2007) 032 [hep-ph/0605296].
- [33] L. T. Wang and I. Yavin, “A Review of Spin Determination at the LHC,” arXiv:0802.2726 [hep-ph].
- [34] See, e.g., A.D. Martin and T.D. Spearman, Elementary particle theory (North-Holland, Amsterdam, 1970) 321 p.
- [35] M. Jacob and G. C. Wick, “On the general theory of collisions for particles with spin,” Annals Phys. **7** (1959) 404 [Annals Phys. **281** (2000) 774].
- [36] G. C. Wick, “Angular momentum states for three relativistic particles,” Annals Phys. **18** (1962) 65.
- [37] S. U. Chung, “Spin Formalisms,” CERN-71-08.
- [38] J. Shelton, “Polarized tops from new physics: signals and observables,” Phys. Rev. D **79** (2009) 014032 [arXiv:0811.0569 [hep-ph]].
- [39] V. Arunprasath, R. M. Godbole and R. K. Singh, “Polarization of a top quark produced in the decay of a gluino or a stop in an arbitrary frame,” Phys. Rev. D **95** (2017) no.7, 076012 [arXiv:1612.03803 [hep-ph]].
- [40] A. Velusamy and R. K. Singh, “Polarization of a vector boson produced in decay of a heavy fermion in an arbitrary frame,” Phys. Rev. D **98** (2018) no.5, 053009 [arXiv:1805.00876 [hep-ph]].
- [41] S. Y. Choi, “Z-boson polarization as a model-discrimination analyzer,” Phys. Rev. D **98** (2018) no.11, 115037 [arXiv:1811.10377 [hep-ph]].
- [42] G. Klln, “Elementary particle physics,” Addison-Wesley, USA (1964) 546p.
- [43] M. E. Rose, “Elementary theory of angular momentum,” New York, United States: Dover Publication Inc. (2011) 272 p.

- [44] S. L. Glashow, “Partial Symmetries of Weak Interactions,” Nucl. Phys. **22** (1961) 579.
- [45] S. Weinberg, “A Model of Leptons,” Phys. Rev. Lett. **19** (1967) 1264.
- [46] A. Salam, “Weak and Electromagnetic Interactions,” Conf. Proc. C **680519** (1968) 367.
- [47] H. Fritzsch, M. Gell-Mann and H. Leutwyler, “Advantages of the Color Octet Gluon Picture,” Phys. Lett. **47B** (1973) 365.
- [48] S. Schael *et al.* [ALEPH and DELPHI and L3 and OPAL and SLD Collaborations and LEP Electroweak Working Group and SLD Electroweak Group and SLD Heavy Flavour Group], “Precision electroweak measurements on the Z resonance,” Phys. Rept. **427** (2006) 257 [hep-ex/0509008].
- [49] J. H. Kuhn and F. Wagner, “Semileptonic Decays of the tau Lepton,” Nucl. Phys. B **236** (1984) 16.
- [50] R. Alemany, N. Rius, J. Bernabeu, J. J. Gomez-Cadenas and A. Pich, “Tau polarization at the Z peak from the acollinearity between both tau decay products,” Nucl. Phys. B **379** (1992) 3.
- [51] J. H. Kuhn and E. Mirkes, “Angular distributions in semileptonic tau decays,” Phys. Lett. B **286** (1992) 381.
- [52] J. H. Kuhn and E. Mirkes, “Structure functions in tau decays,” Z. Phys. C **56** (1992) 661 Erratum: [Z. Phys. C **67** (1995) 364].
- [53] M. Davier, L. Duflot, F. Le Diberder and A. Rouge, “The Optimal method for the measurement of tau polarization,” Phys. Lett. B **306** (1993) 411.
- [54] K. Hagiwara, A. D. Martin and D. Zeppenfeld, “Tau Polarization Measurements at LEP and SLC,” Phys. Lett. B **235** (1990) 198.
- [55] M. Tanabashi *et al.* [Particle Data Group], “Review of Particle Physics,” Phys. Rev. D **98** (2018) no.3, 030001.
- [56] S. S. Gershtein and Y. B. Zeldovich, “Meson corrections in the theory of beta decay,” Zh. Eksp. Teor. Fiz. **29** (1955) 698 [Sov. Phys. JETP **2** (1956) 576].
- [57] R. P. Feynman and M. Gell-Mann, “Theory of Fermi interaction,” Phys. Rev. **109** (1958) 193.
- [58] B. K. Bullock, K. Hagiwara and A. D. Martin, “Tau polarization and its correlations as a probe of new physics,” Nucl. Phys. B **395** (1993) 499.
- [59] F. Abe *et al.* [CDF Collaboration], “Observation of top quark production in $\bar{p}p$ collisions,” Phys. Rev. Lett. **74** (1995) 2626 [hep-ex/9503002].
- [60] S. Abachi *et al.* [D0 Collaboration], “Observation of the top quark,” Phys. Rev. Lett. **74** (1995) 2632 [hep-ex/9503003].
- [61] I. I. Y. Bigi, Y. L. Dokshitzer, V. A. Khoze, J. H. Kuhn and P. M. Zerwas, “Production and Decay Properties of Ultraheavy Quarks,” Phys. Lett. B **181** (1986) 157.
- [62] G. L. Kane, G. A. Ladinsky and C. P. Yuan, “Using the Top Quark for Testing Standard Model Polarization and CP Predictions,” Phys. Rev. D **45** (1992) 124.
- [63] G. A. Ladinsky and C. P. Yuan, “A Probe of new physics in top quark pair production at e^-e^+ colliders,” Phys. Rev. D **49** (1994) 4415 [hep-ph/9211272].
- [64] S. Y. Choi and K. Hagiwara, “Probing the top quark electric dipole moment at a photon linear collider,” Phys. Lett. B **359** (1995) 369 [hep-ph/9506430].

- [65] G. Mahlon and S. J. Parke, “Angular correlations in top quark pair production and decay at hadron colliders,” *Phys. Rev. D* **53** (1996) 4886 [hep-ph/9512264].
- [66] S. J. Parke and Y. Shadmi, “Spin correlations in top quark pair production at e^+e^- colliders,” *Phys. Lett. B* **387** (1996) 199 [hep-ph/9606419].
- [67] E. Asakawa, S. Y. Choi, K. Hagiwara and J. S. Lee, “Measuring the Higgs CP property through top quark pair production at photon linear colliders,” *Phys. Rev. D* **62** (2000) 115005 [hep-ph/0005313].
- [68] P. S. Bhupal Dev, A. Djouadi, R. M. Godbole, M. M. Muhlleitner and S. D. Rindani, “Determining the CP properties of the Higgs boson,” *Phys. Rev. Lett.* **100** (2008) 051801 [arXiv:0707.2878 [hep-ph]].
- [69] W. Bernreuther, *J. Phys. G* **35** (2008) 083001 [arXiv:0805.1333 [hep-ph]].
- [70] D. Choudhury, R. M. Godbole, S. D. Rindani and P. Saha, “Top polarization, forward-backward asymmetry and new physics,” *Phys. Rev. D* **84** (2011) 014023 [arXiv:1012.4750 [hep-ph]].
- [71] R. M. Godbole, K. Rao, S. D. Rindani and R. K. Singh, “On measurement of top polarization as a probe of $t\bar{t}$ production mechanisms at the LHC,” *JHEP* **1011** (2010) 144 [arXiv:1010.1458 [hep-ph]].
- [72] A. Prasath V, R. M. Godbole and S. D. Rindani, “Longitudinal top polarisation measurement and anomalous Wtb coupling,” *Eur. Phys. J. C* **75** (2015) no.9, 402 [arXiv:1405.1264 [hep-ph]].
- [73] B. Tweedie, “Better Hadronic Top Quark Polarimetry,” *Phys. Rev. D* **90** (2014) no.9, 094010 [arXiv:1401.3021 [hep-ph]].
- [74] R. M. Godbole, G. Mendiratta and S. Rindani, “Looking for bSM physics using top-quark polarization and decay-lepton kinematic asymmetries,” *Phys. Rev. D* **92** (2015) no.9, 094013 [arXiv:1506.07486 [hep-ph]].
- [75] L. M. Sehgal and P. M. Zerwas, “ELECTROWEAK gamma Z W INTERFERENCE ON TOPONIUM,” *Nucl. Phys. B* **183** (1981) 417.
- [76] S. Y. Choi, A. Djouadi, M. Guchait, J. Kalinowski, H. S. Song and P. M. Zerwas, “Reconstructing the chargino system at e^+e^- linear colliders,” *Eur. Phys. J. C* **14** (2000) 535 [hep-ph/0002033].
- [77] M. Perelstein, M. E. Peskin and A. Pierce, “Top quarks and electroweak symmetry breaking in little Higgs models,” *Phys. Rev. D* **69** (2004) 075002 [hep-ph/0310039].
- [78] G. Cacciapaglia, A. Deandrea, D. Harada and Y. Okada, “Bounds and Decays of New Heavy Vector-like Top Partners,” *JHEP* **1011** (2010) 159 [arXiv:1007.2933 [hep-ph]].
- [79] C. X. Yue, L. H. Wang and J. Wen, “Single production of heavy top quark from the three-site Higgsless model,” *Chin. Phys. Lett.* **25** (2008) 1613 [arXiv:0708.1225 [hep-ph]].
- [80] T. Han, “The ‘Top Priority’ at the LHC,” *Int. J. Mod. Phys. A* **23** (2008) 4107 [arXiv:0804.3178 [hep-ph]].
- [81] H. C. Cheng, I. Low and L. T. Wang, “Top partners in little Higgs theories with T-parity,” *Phys. Rev. D* **74** (2006) 055001 [hep-ph/0510225].
- [82] M. Schmaltz and D. Tucker-Smith, “Little Higgs review,” *Ann. Rev. Nucl. Part. Sci.* **55** (2005) 229 [hep-ph/0502182].
- [83] K. Agashe, R. Contino and A. Pomarol, “The Minimal composite Higgs model,” *Nucl. Phys. B* **719** (2005) 165 [hep-ph/0412089].
- [84] M. Schmaltz, *JHEP* **0408** (2004) 056 [hep-ph/0407143].

- [85] T. Han, H. E. Logan, B. McElrath and L. T. Wang, “Phenomenology of the little Higgs model,” *Phys. Rev. D* **67** (2003) 095004 [hep-ph/0301040].
- [86] H. Zhou and N. Liu, “Polarization of top quark in vector-like quark decay,” arXiv:1901.02300 [hep-ph].
- [87] J. M. Cornwall, D. N. Levin and G. Tiktopoulos, “Derivation of Gauge Invariance from High-Energy Unitarity Bounds on the s Matrix,” *Phys. Rev. D* **10** (1974) 1145 Erratum: [*Phys. Rev. D* **11** (1975) 972].
- [88] C. E. Vayonakis, “Born Helicity Amplitudes and Cross-Sections in Nonabelian Gauge Theories,” *Lett. Nuovo Cim.* **17** (1976) 383.
- [89] T. D. Lee, “A Theory of Spontaneous T Violation,” *Phys. Rev. D* **8** (1973) 1226.
- [90] G. C. Branco, P. M. Ferreira, L. Lavoura, M. N. Rebelo, M. Sher and J. P. Silva, “Theory and phenomenology of two-Higgs-doublet models,” *Phys. Rept.* **516** (2012) 1 [arXiv:1106.0034 [hep-ph]].